

APPROVED FOR PUBLIC RELEASE,  
DISTRIBUTION IS UNLIMITED

19980105 066

# REPORT DOCUMENTATION PAGE

*Form Approved  
OMB No. 0704-0188*

Public reporting burden for this collection of information is estimated to average 1 hour per response, including the time for reviewing instructions, searching existing data sources, gathering and maintaining the data needed, and completing and reviewing the collection of information. Send comments regarding this burden or any other aspect of this collection of information, including suggestions for reducing this burden, to Washington Headquarters Services, Directorate for Information Operations and Reports, 1215 Jefferson Davis Highway, Suite 1204, Arlington, VA 22202-4302, and to the Office of Management and Budget, Paperwork Reduction Project (0704-0188), Washington, DC 20503.

<b>1. AGENCY USE ONLY (Leave blank)</b>			<b>2. REPORT DATE</b> October 1997		<b>3. REPORT TYPE AND DATES COVERED</b> Contract Report		
<b>4. TITLE AND SUBTITLE</b>  Validation of Acoustic Measurements of Wind and Precipitation using Expendable Ambient Noise Sensor (ANS) Drifters, AN/WSQ-6 (XAN-2)			<b>5. FUNDING NUMBERS</b>  Job Order No. 74-5136-07 Program Element No. 0604218N		<b>6. AUTHOR(S)</b>  Jeffrey A. Nystuen		
<b>7. PERFORMING ORGANIZATION NAME(S) AND ADDRESS(ES)</b>  Applied Physics Laboratory University of Washington Seattle, Washington			<b>8. PERFORMING ORGANIZATION REPORT NUMBER</b>  NRL/CR/7406--97-0012		<b>9. SPONSORING/MONITORING AGENCY NAME(S) AND ADDRESS(ES)</b>  Naval Research Laboratory Center for Tactical Oceanographic Warfare Stennis Space Center, MS 39529-5004		
<b>11. SUPPLEMENTARY NOTES</b>  In support of Basic Contract No. N00014-94-1-G906							
<b>12a. DISTRIBUTION/AVAILABILITY STATEMENT</b>  Approved for public release, distribution is unlimited.				<b>12b. DISTRIBUTION CODE</b>			
<b>13. ABSTRACT (Maximum 200 words)</b>  Air-deployable autonomous drifters have been developed to monitor upper ocean environmental conditions in remote or difficult regions. One version of these drifters (AN/WSQ-6 series, model XAN-2) includes ambient noise measurements in 16 frequency bands from 5 Hz to 25 kHz. One application of this sensor is the passive identification and analysis of local weather conditions. This analysis is possible because breaking waves, related to wind speed or sea state, and precipitation produce loud and unique sound underwater. This report describes the performance of 15 of these ambient noise sensor (ANS) drifters deployed in a variety of water conditions at various locations around the world. Acoustically derived present weather conditions are compared with the Defense Meteorological Satellite Program (DMSP) passive microwave sensor (SSM/I) images. While regional variations in the high frequency (25 kHz) sound spectrum were observed, the acoustic measurement of wind speed using 8 kHz sound levels did not show regional or environmental variability. Overall, the correlation between the ANS and SSM/I wind speed measurements is 0.91. Acoustically detected precipitation is verified by the SSM/I sensors in 19 of 21 events (90.5%). The ANS drifters did not detect light rain/drizzle when the wind speed was greater than 10 m/s.							
<i>DTIC QUALITY INSPECTED</i>							
<b>14. SUBJECT TERMS</b> acoustics, air-deployable drifters, ambient noise, meteorology, wind speed, sea state, DMSP, SSM/I, ANS, AN/WSQ-6, and XAN-2					<b>15. NUMBER OF PAGES</b> 34		
					<b>16. PRICE CODE</b>		
<b>17. SECURITY CLASSIFICATION OF REPORT</b> Unclassified		<b>18. SECURITY CLASSIFICATION OF THIS PAGE</b> Unclassified		<b>19. SECURITY CLASSIFICATION OF ABSTRACT</b> Unclassified		<b>20. LIMITATION OF ABSTRACT</b> SAR	

Validation of Acoustic Measurements of Wind and Precipitation

using

Expendable Ambient Noise Sensor (ANS) Drifters, AN/WSQ-6 (XAN-2)

Jeffrey A. Nystuen  
Applied Physics Laboratory  
University of Washington  
Seattle, Washington

Grant # N00014-94-1-G906  
(to the University of Miami)

Prepared for:

Tactical Oceanography Warfare Support Program Office  
Code 7410  
Naval Research Laboratory  
Stennis Space Center, MS 39529-5004

October 24, 1997

Validation of Acoustic Measurements of Wind and Precipitation  
using  
Expendable Ambient Noise Sensor (ANS) Drifters, AN/WSQ-6 (XAN-2)

Jeffrey A. Nystuen  
Applied Physics Laboratory  
University of Washington  
Seattle, Washington

**Abstract:**

Air-deployable autonomous drifters have been developed to monitor upper ocean environmental conditions in remote or difficult regions. One version of these drifters (AN/WSQ-6 series, model XAN-2) includes ambient noise measurements in 16 frequency bands from 5 Hz to 25 kHz. One application of this sensor is the passive identification and analysis of local weather conditions. This analysis is possible because breaking waves, related to wind speed or sea state, and precipitation produce loud and unique sound underwater. This report describes the performance of 15 of these ambient noise sensor (ANS) drifters deployed in a variety of water conditions at various locations around the world. Acoustically derived present weather conditions are compared the Defense Meteorological Satellite Program (DMSP) passive microwave sensor (SSM/I) images. While regional variations in the high frequency (25 kHz) sound spectrum were observed, the acoustic measurement of wind speed using 8 kHz sound levels did not show regional or environmental variability. Overall, the correlation between the ANS and SSM/I wind speed measurements is 0.91. Acoustically detected precipitation is verified by the SSM/I sensors in 19 of 21 events (90.5%). The ANS drifters did not detect light rain/drizzle when the wind speed was greater than 10 m/s.

## **1. Introduction**

Expendable, air-deployable drifters have recently been developed to provide real-time measurements of upper ocean conditions (Selsor, 1993). These drifters, designated AN/WSQ-6 series by the Navy, provide conventional measurements of air-sea temperatures, atmospheric pressure and ambient noise levels. In addition, the interpretation of the high frequency ( $> 500$  Hz) ambient sound data can be used to detect local weather conditions and to quantify wind speed and rainfall rate. This report compares these acoustically derived present weather condition measurements with co-located passive microwave satellite measurements.

## **2. Background**

Sources of the ambient sound field in the ocean have been explored for years (Wenz, 1962). Above 500 Hertz, the principal physical sources are 1) waves breaking due to wind and changing seas and 2) precipitation including drizzle and heavy rain. The sound field is further modified by the presence of ambient sub-surface bubbles (Farmer and Lemon, 1984). In each situation, the sound field is distinctive, allowing acoustic identification of surface conditions (Nystuen and Selsor, 1997). In particular four weather classifications: wind without ambient bubbles present, wind with ambient bubbles present, drizzle and heavy rain, can all be identified and quantified acoustically.

### *a) wind only, no ambient bubbles*

Starting at a wind speed of about 2 m/s, wind generates sound above 500 Hz through breaking waves. The exact mechanism appears to be the initial oscillations of individual bubbles ("active" bubbles versus the "ambient" bubbles which modify the sound field through attenuation) created during wave breaking (Medwin and Beaky, 1989). At lower wind speeds, the distribution of bubble sizes appears to be independent of wind speed, resulting in a relatively uniform sound spectrum shape. This slope of this spectrum has been used to identify the situation "wind only, no ambient bubbles present" (Vagle et al. 1990). However, systematic departures from this slope value have been observed (Dailey, 1991; Nystuen and Selsor, 1997) and so some caution needs to be used.

### *b. wind only, ambient bubbles present*

Once the wind speed exceeds about 10 m/s, wave breaking becomes so extensive that an ambient bubble "layer" forms. In fact, this layer is an ensemble of bubble plumes and clouds. The overall effect on the sound field is to change the shape of the acoustic spectrum (Farmer and Lemon, 1984). Bubbles radiate and absorb sound very efficiently at their resonant frequencies. Newly created bubbles, within the actively breaking wave, radiate sound. But, bubbles mixed down into the water column become quiet and subsequently absorb sound. Large bubbles (1 mm radius) do not remain in the water column very long, whereas small bubbles ( $< 200$  microns radius) can get stirred downward and form an effective bubble layer. This means that newly generated surface sound at higher frequencies (over 10 kHz) is absorbed, while lower frequency sound ( $< 5$  kHz) is not. The slope of the sound spectrum can become very steep, more than -25 dB/decade, especially above 10 kHz. The exact frequency where this phenomena begins to be observed depends on the extent of wave breaking and is therefore wind speed and sea condition dependent. Vagle et al. (1990) suggest a wind dependent "critical" frequency, above which absorption, and therefore spectral shape changes occur.

### *c. drizzle*

Drizzle, or light rain, has a unique spectral signature because of the sound production mechanism of 1 mm diameter raindrops. This drop size is relatively small, and is therefore present in almost all rainfall including very light drizzle. The sound production mechanism is

bubble formation by a "regular" entrainment process (Pumphrey et al. 1989) and produces a characteristic peak in the sound field between 13-20 kHz. Drizzle is detected by listening for excess sound in the 13-20 kHz spectral band relative to the sound energy in a lower frequency band, e.g. 5 kHz. The mechanism is sensitive to wind (Nystuen, 1993) and, in fact, no "drizzle" signatures, spectral "peaks", are detected when the wind speed exceeds 10 m/s. On the other hand, the drizzle signature is detected for wind speeds of order 5 m/s, a higher wind speed than previously anticipated.

#### *d. heavy rain*

The "regular entrainment" mechanism responsible for sound production by small drops breaks down for drops larger than 1.1 mm diameter. The next size category, medium drops from 1.2 - 2.0 mm diameter, are relatively quiet acoustically and therefore hard to measure (Nystuen, 1996). But larger raindrops, over 2 mm diameter, have energetic enough splashes so that bubbles are again formed underwater during the splash (Medwin et al., 1992). Once these drops are present, the rainfall rate is usually moderate to heavy (over 2 mm/hr). The distribution of bubble sizes formed by the larger raindrop splashes includes larger bubbles than those that are associated with small raindrops, and thus the lower frequency sound intensities are elevated as well as higher frequencies. Furthermore, the distribution of bubbles sizes does not match that of breaking waves, and so the shape of the sound spectrum is unique and allows "heavy rain" to be detected. The influence of high wind on this sound production mechanism has not been fully studied. Nystuen et al. (1993) did not observe a strong wind dependence and Nystuen and Farmer (1989) detected rain even under relatively high wind conditions (order 15+ m/s).

## **2. Drifting Buoy Description**

The naval designation for the drifting buoys used in this study is AN/WSQ-6 series, model XAN-2, ambient noise sensor (ANS) drifters (Selsor, 1993). These buoys fit inside a standard A-size sonobuoy canister. They are certified to be air deployed using a standard sonobuoy chute from aircraft. As the canister leaves the airplane, the end cap is pulled off and a parachute deploys. Upon contact with sea water, the sea water electrode triggers the gas cylinders to discharge, inflating the floatation collar, deploying the antenna and dropping the hydrophone package (hydrophone, drogues, weight and cable). The physical configuration of a deployed buoy is shown in Fig. 1. Geophysical sensors include a hydrophone, thermistors and a barometer.

The drogues are designed to decouple the motion of the surface buoy from the hydrophone, located at the lowest drogue. This is required to reduce flow noise, which would be detected as noise at frequencies below 100 Hz. The drogues produce a 17:1 drogue/cable to surface buoy drag ratio, thus providing limited Lagrangian drifter characteristics.

The pressure sensor is a low-cost, temperature compensated strain gauge with dynamic range 850-1054 mb  $\pm$  1 mb (McCormick et al., 1990). The pressure port, covered with a Gore-Tex splash guard, is at the top of the antenna mast to reduce problems with splash and submergence. The strain gauge itself is located at the bottom of the drifter hull, below the water line, to improve temperature stability.

The air temperature sensor, shielded from direct sun, is located near the top of the mast. It has a range of -30° to 46°C  $\pm$  0.2°C. The surface water temperature sensor is incorporated into the base of the buoy hull. Its range and sensitivity is -5 to +35°C  $\pm$  0.2°C. Performance characteristics were verified by McCormick et al. (1990).

The ambient sound sensor is an omni-directional ( $\pm$  1 dB below 10 kHz;  $\pm$  3 dB from 10-25 kHz) hydrophone located at the lowest drogue at 100 m depth. The underwater sound field is sampled once per hour through 16 third octave band pass filters with center frequencies from 5 Hz to 25 kHz. The signal from each third octave filter is converted to a DC voltage using a root mean square circuit and is digitized using a 16-bit analog-digital circuit. The resulting dynamic range is 9

orders of magnitude in acoustic intensity ( $35 - 125 \text{ dB} \pm 2 \text{ dB}$  relative to  $1 \mu\text{Pa}^2/\text{Hz}$  from 5 Hz to 5 kHz and  $20 - 110 \text{ dB} \pm 2 \text{ dB}$  relative to  $1 \mu\text{Pa}^2/\text{Hz}$  from 8 kHz to 25 kHz).

Data from the pressure, temperature and ambient sound sensors are stored in six 32-bit data blocks and broadcast by the ARGOS satellite transmitter every 90 seconds. Depending on the buoy latitude, satellites are in position to receive the ARGOS transmission 8-12 times per day. The ambient noise data are sampled and updated once per hour while data from the other sensors are sampled and updated every 10.5 minutes. Only the latest data are transmitted.

Examples of individual sound spectra are shown in Fig. 2. Several features of "wind only" spectra are shown. Under moderate wind conditions, 4-10 m/s in this example, the shape of the sound spectra are the same. This spectral shape allows "wind only" conditions to be detected. Strict dependence on spectral slope to detect "wind only" conditions fails under the other two examples shown here. For calm conditions, labeled background, there is no wind generated sound and thus the shape of the sound spectrum is noise, and is therefore unpredictable. In this case, the spectral slope becomes white above 5 kHz. At the other extreme is the "very high seas" situation. If the wind is extremely high, in this case over 15 m/s, bubbles entrained in the surface layer from breaking waves attenuate high frequency sound resulting in a very steep spectral slope. Three weather conditions appear to generate this phenomena: very high winds; rain in the present of high winds; and winds blowing against existing seas.

Three rainfall detections are also shown in Fig. 2. Spectrum r1 is a light drizzle showing the characteristic spectral peak between 13-20 kHz associated with small raindrops. Spectrum r2 is light rain under moderate wind conditions, roughly 7 m/s based on the match to the 7 m/s "wind only" spectrum. The whiter spectrum between 5-15 kHz suggests that larger drops are also present. Note that the spectral "peak" is no longer a peak but rather relatively more energy in the 13-20 kHz band. This is because of the known influence of wind to suppress the sound production mechanism for small (0.8-1.1 mm) drops typical in light rain. In this case, the acoustic rainfall rate estimate is 1.4 mm/hr while the concurrent microwave satellite estimate is 2 mm/hr.

Spectrum r3 is a heavy rainfall detection recorded during rapidly rising wind conditions, probably 10-12 m/s. Again, no "peak" is evident in the sound spectrum, however relatively more high frequency energy is present allowing acoustic detection of rain. The acoustic rainfall rate is 8 mm/hr; the microwave satellite rainfall rate is 3 mm/hr. In the case of heavy rain during high winds, changes to the spectral shape are subtle. Thus, strict dependence on the spectral slope for determining weather classification is risky. A more reliable method is to compare the sound levels at a lower frequency, e.g. 5 kHz, with those at a high frequency, e.g. 25 kHz (Fig. 3). The "wind only" points cluster into a well defined group. Departures from this locus allow the detection of rain, drizzle, high seas and shipping (Nystuen and Selsor, 1997). A second related clustering method which shows promise for weather classification is the comparison of high frequency (8-25 kHz) spectral slope and the sound level at 5 kHz (Fig. 4).

### 3. Comparison data - DMSP SSM/I passive microwave fields

In situ data at remote ocean locations is relatively difficult to obtain. This is especially true for precipitation where even moored buoys have been unable to provide reliable data. In contrast, satellites have been scanning the oceans for years. The satellite sensors span the electromagnetic spectrum and are used to measure an amazing variety of geophysical fields. The frequencies used to measure the different geophysical field depend on the emissive, reflective and scattering properties unique to the desired field (see e.g., Stewart 1985). The fields of interest in this report include surface wind speed, cloud liquid water and precipitation. Indirect measurements of these fields are often possible using visible and infrared frequencies, however clouds often obscure the scene. In the microwave frequency band, clouds are relatively transparent. Thus, direct measurements of surface emission are possible. Surface emission is

related to surface wind speed through wave breaking/surface roughness. Absorption, emission and scattering by liquid particles (cloud and rain droplets) in the air allows cloud liquid water (precipitable water) and rainfall to be measured directly. Operational algorithms for the measurement of wind speed (Wentz, 1994) and cloud liquid water (Weng and Grody, 1994) exist. Algorithm development for precipitation is ongoing (e.g., Barrett et al. 1994). The drawback of the microwave algorithms is the poor spatial resolution (15-50 km depending on frequency) and the poor temporal resolution (order 12 hours).

The wind speed algorithm used here is from Goodberlet et al. (1990). This algorithm was empirically derived using moored buoy anemometer winds. The wind speed algorithm is only valid away from precipitation or frontal regions. These conditions are detected using total cloud liquid water (cloud and rain drops). If cloud liquid water is above a threshold of  $0.2 \text{ kg/m}^2$  ( $0.2 \text{ mm}$  depth), then the wind speed measurement is assumed to be affected, usually by overestimation of wind speed (Ferraro et al., 1996). This is due to absorption/emission from the liquid water drops in the intervening clouds. An algorithm for cloud liquid water (Weng and Grody, 1994) is used to flag the SSM/I wind speed measurements. While high cloud liquid water values do not necessarily imply rain at the surface, high values will be used to "detect" drizzle or rain present at the surface. If the rain algorithm, to be described below, measures less than 1 mm/hr, then "drizzle" rather than "heavy rain" is assumed to be present.

Microwave rainfall rate algorithms exist but are generally not verified. This is because of the difficulty of obtaining in situ rainfall measurements. The algorithms are physically based, rather than empirically determined. The one used here is from Wilheit et al. (1991). One consideration in the model is the atmospheric freezing level. This is because frozen particles do not radiate as much energy as liquid particles at microwave frequencies. Given the sea surface temperature (SST), the freezing level can be estimated using a standard lapse rate of  $-6.5 \text{ }^\circ\text{C/km}$ . The estimate of precipitation rate is further compromised by realizing that the spatial scale of rainfall is much smaller than the spatial resolution of the satellite. This is especially true for the intense convective rainfall often associated with precipitation in tropical and sub-tropical regions. For wide-spread "stratiform" rainfall associated with mid-latitude frontal systems, this problem is still present, but less severe.

The microwave satellite data available for comparison comes from the Defense Meteorological Satellite Program (DMSP) satellites F-10 and F-13. These satellites carry Special Sensor Microwave Imagers (SSM/I), passive microwave sensors. Data are available from the NASA Marshall Space Flight Center's Global Hydrology and Climate Center. High density tapes of daily individual orbits were acquired. These data were processed to extract the data in a  $3^\circ$  by  $3^\circ$  region surrounding the individual drifters. The data were then processed to brightness temperature values, which, in turn, are the inputs into the various geophysical algorithms described above.

#### 4. Description of the data

The Tactical Oceanography Warfare Support (TOWS) program office of the Naval Research Laboratory - Stennis Space Center (NRL-SSC) oversaw development of the ANS drifters (Selsor, 1993). As part of this development program, drifters were deployed in a wide variety of locations and water conditions. Several of the drifters described herein were deployed specifically as part of this evaluation effort (#14267-72, #14275), while others (#14259, #26304-#26308) were deployed as part of Navy fleet exercises. Thus, there is a high potential for unusual ship activity, including sonar pings at unusual frequencies, near this later set of drifters. Table 1 shows a summary of drifters used in this assessment of performance. Several additional drifters were also deployed, but failed on launch or did not report usable acoustic data.

Table 1. Acoustic Drifter Deployments

<u>ID number</u>	<u>location</u>	<u>Deployment date</u>	<u>latitude/longitude</u>
#14259	Hawaii	128-130 1996 (May 7-May 9)	16-17N 154-155W
#14269	E N Pacific	86-96 1996 (Mar 26 - Apr 5)	47-48N 128-130W
#14270	E N Pacific	87-103 1996 (Mar 27 - Apr 12)	44-46N 127-129W
#14272	E N Pacific	86-96 1996 (Mar 25 - Apr 5)	47-48N 129-130W
#14271	W N Atlantic	262-267 1995 (Sep 19-Sep 24)	28-30N 68-70 W
#26304	W N Pacific	72-78 1996 (Mar 12-Mar 18)	40-42N 143-145E
#26305	W N Pacific	72-82 1996 (Mar 12-Mar 22)	44-45N 152-153E
#26306	W N Pacific	73-91 1996 (Mar 13-Mar 31)	39-40N 135-136E
#26307	W N Pacific	73-116 1996 (Mar 13-Apr 25)	34-38N 130-133E
#26308	E N Atlantic	134-144 1996 (May 13-May 23)	61-63N 2-5 W
#14268	W N Atlantic	339-344 1995 (Dec 5-Dec 10)	27-28N 79-80W
#14275	G Mexico	55-63 1996 (Feb 24 - Mar 2)	24-25N 92-93W

*a. Drifter #14259 - near Hawaii*

This was a short-lived deployment under warm water, calm seas conditions. Only 3 SSM/I images were available for comparison to the ANS drifter data. No precipitation was detected using the satellite sensor. One possible "drizzle" detection was detected acoustically. Anomalous manmade noise at 200 and 500 Hz was present during this deployment (Curtis, pers. comm., 1997). The cause of buoy failure is unknown.

*b. Drifters #14269, 14270 and 14272 - Eastern North Pacific Ocean*

These three drifters were deployed off the coast of Washington in May 1996 (Fig. 5). The atmospheric pressure and temperature records from the three drifters are shown in Fig. 6. There is close agreement between the drifters, although Drifter #14270 is in warmer water more than 100 km from the other two drifters. Wind speeds measured acoustically and compared to the SSM/I wind speed measurements are shown in Fig. 7. The correlation coefficient between the acoustic and satellite wind speed measurements are 0.93, 0.89 and 0.92, respectively. Fig. 8 shows the rainfall detection and rainfall rate comparisons. Heavy rains on JD 96 (Drifters 14269 and 14272) and on JD 102 (Drifter 14270) are detected by both sensors. Light rain/drizzle is detected by both sensors on JD 91 (Drifter 14272), 92, 97 and 101 (Drifter 14270). Light rain/drizzle is detected by the satellite, but not acoustically on JD 94 and 95. At these times the wind speed is high, of order 10 m/s, and one would expect the acoustic drizzle signal to be minimal. The acoustic rainfall detection on JD 93 (Drifter 14269) is not confirmed by a satellite measurement. Each of these drifters broke during 15 m/s wind conditions.

*c. Drifter #14271 - Western North Atlantic Ocean*

This drifter was deployed in warm water ( $26^{\circ}\text{C}$ ) and lasted 5 days under light wind (< 5 m/s) conditions. Only 3 non-rain SSM/I images are available for comparison. One SSM/I rain detection is not confirmed acoustically, however there is no acoustic measurement within 0.1 days. No SSM/I images are available within 0.3 days of the two acoustic drizzle detections. The cause of drifter failure is unknown.

*d. Drifters # 26304, 26305, 26306 and 26307 - Western North Pacific Ocean near Japan*

These drifters were deployed near Japan in March 1996 (Fig. 9). Two (Drifters 26304 and 26305) were in cold water ( $0\text{-}1.5^{\circ}\text{C}$ ) northeast of Japan (Fig. 10). The wind speed comparisons with the SSM/I are very good, correlation coefficients of 0.95 and 0.90, respectively (Fig. 11). One drizzle and two light rainfall events were detected acoustically for Drifter #26304 (Fig. 12). The drizzle event at JD 75.8 and the rainfall event at JD 76.2 were not detected with the SSM/I, although at JD 75.5 (the closest temporal image) there was precipitation in the vicinity of the drifter. The next available SSM/I image occurred at JD 76.5. This points out the difficulty with temporal resolution using the SSM/I sensor. The third event at JD 77.3 was detected as heavy rain by both the SSM/I (8 mm/hr) and the ANS Drifter (2-4 mm/hr). There were no precipitation detections by either type of sensor for Drifter #26305.

Drifter #26305 also produced a high wind speed correlation (0.90) when compared to the SSM/I sensors (Fig. 11), however there were two data anomalies. First, the sound levels at 25 kHz are approximately 8 dB higher than the levels reported by any other drifter (Fig. 13). This required that the weather classification algorithm be rewritten specifically for this drifter. Higher levels are also present at 20 kHz (4 dB) and at 14.5 kHz (2 dB). The magnitude of these anomalies is very large, well outside of the required tolerances of the instrument, and thus suggests that the high frequency sound levels at this ocean location are really present! No confirmation of this fact is available. This high frequency sound anomaly does not appear to affect the acoustic wind speed measurements (Fig. 11).

Near the end of the deployment for Drifter #26305, at JD 81.3, the sound levels at all frequencies from 5 Hz to 25 kHz increased by 8-20 dB (Fig. 14). This anomaly, especially large at 5 Hz, suggests that the drifter was snagged, perhaps by a ship. Few sound sources span such a large range of frequencies. Possible naval operations in the near vicinity of the drifter could also be responsible for this anomaly. The weather classification algorithm falsely interpreted this condition as extremely heavy rainfall.

Drifters #26306 and #26307 were deployed in warmer water west of Japan (Fig. 9). These were the two longest lived drifters, 19 and 43 days, respectively. The environmental data is shown in Fig. 15 and the wind speed measurement comparisons are shown in Fig. 16. Rainfall detection is shown in Fig. 17. Seven of nine events are detected by both sets of sensors. Two events, one at JD 81.5 (Drifter #26306) and one at JD 104 (Drifter #26307) are not detected by the SSM/I. In both cases, the rain appeared to occur in between successive SSM/I images (Fig. 18). Note, in particular, the close agreement between the acoustic and satellite wind measurements just prior to and just after the rain at JD 104.0 for Drifter #26307. Apparently, this rain event had a very short temporal scale. The temporal resolution of the satellites was not sufficient to detect these two events.

*e. Drifter # 14268*

Drifter #14268 was deployed in shallow water north of the Bahamas. It became grounded, apparently on coral reef. The sound field in shallow warm water locations is often dominated by snapping shrimp. These creatures have a maximum in their acoustic field at 3-10

kHz. The sound spectrum from Drifter #14268 shows this characteristic shape (Fig. 19) and thus it is assumed that the acoustic data is contaminated by snapping shrimp sound.

*f. Drifter #14275 - Gulf of Mexico*

This drifter was deployed in the Gulf of Mexico. Wind speed correlation between the SSM/I and ANS sensor is high (0.92), but rainfall rate confirmation is poor (Fig. 20). An acoustic rainfall detection occurred at 58.4 which was not detected by the SSM/I at 58.48. However, that SSM/I wind speed at 58.48 (11.2 m/s) was very high relative to the ANS wind speed at 58.52 (7.9 m/s), suggesting that rainfall contamination (sub-resolution) in the SSM/I field may have been present. The other ANS rainfall detection at 59.5 was also missed by the SSM/I, however there were no SSM/I images within 0.2 days of the ANS rainfall detection. SSM/I drizzle detections occurred on JD 62. During these times, the ANS record shows high seas and 10 m/s winds. Drizzle is unlikely to be detected acoustically under such conditions. The cause of drifter failure is unknown.

*g. Drifter #26308 - north of Scotland*

This drifter was deployed north of Scotland and drifted steadily westward during its 11 days of operation. The wind speed comparison between the drifter and the satellites (Fig. 21) is the poorest of all drifters ( $r = 0.56$ ), however an anomalous peak at 4 kHz is present in the sound spectrum between JD 142.4 and 143.6. During this period that the ANS wind speeds estimates are significantly higher than the SSM/I wind speeds, suggesting that the peak is a noise feature contaminating the sound field. A possible source is naval sonars, as this drifter was deployed during naval exercises. This noise feature is not detected by the classification algorithm. After removing these noise points, the comparison improves to a correlation coefficient of  $r = 0.83$ .

Between JD 136-138, the SSM/I wind speed estimates are significantly higher than the ANS measurements. During this period the air temperature was 3-5 °C colder than the sea surface temperature (Fig. 21), implying unstable boundary layer conditions. The sound levels below 500 Hz were depressed 10 dB relative to the rest of the deployment (poor surface sound duct).

There is only one precipitation detection for this buoy. It is a drizzle detection and occurs on JD 141.3 and is detected by both instruments, although the wind speed is nearly 10 m/s.

*h. Drifters # 14267, #14273 and #14276*

Data from these drifters were not used. In the case of #14267 and #14273, the deployments were too short (3 days each) to accumulate sufficient SSM/I data for intercomparisons. Both were deployed in warm water, Gulf of Mexico and Gulf Stream, respectively. The cause of drifter failure is unknown. The acoustic data from #14276 were noisy throughout its deployment (over 60 days) and were unusable.

*i. Summary*

The following tables summarize the drifter deployment statistics. Table 2 shows the drifter lifetime statistics. The specific cause of each drifter failure is unknown as none of the drifters were recovered for inspection, however the general weather conditions can be estimated from the acoustic (or satellite) measurements just prior to failure. An interesting observation is that all of the warm water (over 20°C) drifters failed within 7 days of deployment in apparently benign conditions (low wind/sea state). In contrast, all of the cooler water drifters lasted more than 7 days and failed under rough conditions (high winds/sea state). The mean lifetime of the

buoys was 11 days. For the warm water drifters, the mean lifetime was 4.3 days and for the cool water drifters, the mean lifetime was 16 days.

Table 2. Drifter lifetime

<u>Drifter #</u>	<u>lifetime (days)</u>	<u>apparent failure</u>	<u>water temperature</u>
14259	3	unknown	warm
14269	11	high winds	cool
14270	16	high winds	cool
14272	11	high winds	cool
14271	5	unknown	warm
14275	7	unknown	warm
14268	5	coral reef	warm
14267	3	unknown	warm
14273	3	unknown	warm
26304	7	high winds	cold
26305	10	high winds	cold
26306	19	high winds	cool
26307	43	high winds	cool
26308	11	high winds	cool
14276	--	bad acoustics	

Table 3 summarizes the wind speed measurement comparison between the ANS drifters and the SSM/I sensors. Overall, 154 days of ANS drifter data are available for comparison. A total of 254 rain-free SSM/I images were matched to these data. The overall correlation is 0.91 (Fig. 22). A linear regression curve through these data shows a slope of 0.98 and an offset of 0.8 m/s, with the SSM/I wind speed measurements higher than the ANS measurements by 0.8 m/s. This result is nearly identical to the observations of Nystuen and Selsor (1997). No trends based on the available environmental data, e.g., sea surface temperature, or by region are apparent in these data.

Table 3. Wind Speed Measurement Comparisons

<u>Drifter #</u>	<u>lifetime(days)</u>	<u># SSM/I images</u>	<u>mean SST</u>	<u>correlation</u>
14259	3	3	27 °C	0.86
14269	11	21	8-9 °C	0.93
14270	16	24	10 °C	0.89
14272	11	15	8 °C	0.92
14271	5	3	26 °C	-0.5
14275	7	14	23 °C	0.92
26304	7	13	0 °C	0.95
26305	10	25	1.5 °C	0.90
26306	19	37	5-7 °C	0.93
26207	43	73	12-13 °C	0.90
26308	11	26	8 °C	0.83
TOTAL	154	254	-----	0.91

A summary of rainfall detection is shown in Table 4. The data are separated by rainfall intensity: drizzle (< 1 mm/hr) and heavier rain (> 1 mm/hr). In each case, the number of detections for each sensor (acoustic or SSM/I) are given together with the number of these

detections that were also detected by the other sensor, i.e. 3/1 under SSM/I means 3 detections by the SSM/I sensor with one of the events detected by the ANS drifter. A drizzle detection by the SSM/I sensor is assumed if the cloud liquid water measurement is over  $0.2 \text{ kg/m}^2$  (Ferraro et al., 1996), but the rainfall rate measurement (Wilheit et al. 1991) is below 1 mm/hr. There were a total of 13 SSM/I images where drizzle was detected. Of these, just 6 (46%) were also detected acoustically. Six of the seven missed detections occurred under high wind ( $> 10 \text{ m/s}$ ) conditions, indicating that the acoustic detection of drizzle is not likely under high wind speed conditions. The ANS drifters detected drizzle 8 times. Of these, 6 events were confirmed by the SSM/I sensors. The two "misses" had no SSM/I images within 0.2 days of the acoustic detections. There were 14 SSM/I rainfall detections; 11 of these were confirmed acoustically (85%). Two of the "misses" occurred during high wind conditions and the other miss had no acoustical measurement within 0.1 days of the SSM/I image. Finally, the ANS sensors detected rain 19 times. Thirteen of these events (68%) were confirmed by the SSM/I sensors, however 4 of the 6 "misses" were apparently due to the poor temporal resolution of the satellite data. Eliminating "misses" due to poor temporal sampling by the satellites, 13 of 15 (87%) of the "heavy rain" events and 19 of 21 (90.5%) of all precipitation events detected acoustically were confirmed by SSM/I observations.

Table 4. Rainfall Detection

Drifter #	Drizzle (< 1 mm hr)		Rain (> 1 mm hr)	
	SSM/I	ANS	SSM/I	ANS
14259	0/0	0/0	0/0	0/0
14269	3/0	0/0	1/1	3/2
14270	3/2	3/3	3/2	2/2
14272	3/1	1/1	3/2	2/2
14271	0/0	2/0	1/0	0/0
14275	1/0	0/0	0/0	2/0
26304	0/0	0/0	1/1	2/1
26305	0/0	0/0	0/0	0/0
26306	0/0	0/0	2/2	3/2
26307	2/2	1/1	3/3	5/4
26308	1/1	1/1	0/0	0/0
total	13/6	8/6	14/11	19/13

## 5. Discussion

### a. Weather Classification

Variations in the shape of the scatter diagram existed for different sets of drifters. This was due to regional variations in the ambient sound field at 25 kHz. In particular, the three drifters in the Eastern North Pacific (#14269, #14270 and #14272) had slightly lower ambient sound levels at 25 kHz, while Drifter #26305 (northeast of Japan) had extremely high ambient sound levels at 25 kHz, relative to the other drifters (Fig. 13). These apparent regional variations in the sound field required that the weather classification algorithm described by Nystuen and Selsor (1997) be modified. In particular, by using lower frequencies (4 and 20 kHz, rather than 5 and 25 kHz, the only drifter exhibiting an ambient sound anomaly was #26305. The modified weather classification algorithm is given in the Appendix.

An alternate measure of weather classification is the spectral slope measurement (Vagle et al. 1990). While this measure appears promising, its application proved difficult. Instrument or regional variations affect this measurement. Furthermore, unpredictable values at very low

wind speed, the "true" background noise spectrum, make classification using this measure alone risky. Nevertheless, there is evidence that this measure can be used in conjunction with the other measures to identify weather classifications (Fig. 4). Ultimately, a composite algorithm is likely to be useful.

#### *b. Wind Speed Comparisons*

Overall, the wind speed comparison between the SSM/I and the ANS drifters is very good (254 data points; correlation coefficient of 0.91). No anomalies based on available environmental factors, in particular, sea surface temperature, were detected. Furthermore, the regional variations in high (25 kHz) frequency sound levels noted above do not appear to affect the wind speed measurement. The Vagle et al. (1990) algorithm is applied at 8 kHz.

#### *c. Rainfall Detection*

The detection and measurement of rainfall at sea has many potential applications. This include the direct measurement of rainfall for climatological data bases, as well as real time detection as input into mixed layer, aerosol production, visibility and communication models. Validation of rainfall measurements is difficult because of the lack of good *in situ* techniques for rainfall measurement and the inherent spatial and temporal discontinuity of rainfall. In these data, the comparison of rainfall detection is promising, but difficult to fully evaluate. The SSM/I sensors detected precipitation 27 times, although "drizzle" detection (13 times) by the SSM/I is highly speculative (based on total cloud liquid water values). Of these precipitation events, 17 were also detected acoustically. Of the missed events, 8 of 10 were under light rain/high wind conditions when the physical mechanism for sound generation by small raindrops is known to break down. One other event was apparently missed because of temporal sampling mismatch between the ANS drifter and the satellite sensors.

The ANS drifters also detected precipitation 27 times. Nineteen of these events were confirmed by the SSM/I sensor. Most of the "misses" were due to inadequate temporal sampling by the satellite sensors. If temporal sampling is eliminated by requiring that the comparison occur only when SSM/I images and ANS data are within 0.1 days, then the comparison success improved to 19 of 21 ANS detections (90.5%). Using only events which were detected by both types of sensors, a comparison of rainfall rates produced at correlation coefficient of 0.34. While this is a low correlation coefficient, it is not an unexpectedly low value given the mismatch in temporal and spatial scales of the sensors and the short temporal and spatial scales of rainfall.

False acoustic detections of rainfall are a potential problem. This occurred twice with these data (Drifter #26305 and #26308). In both cases, further examination of the low frequency (below 500 Hz) sound levels revealed suspect (i.e., likely contaminated) acoustical data. The classification algorithm did not initially identify these two situations. It should be noted that both of these buoys were deployed as part of "fleet exercises" and therefore may have been exposed to unusual local shipping or naval "sonar" noise.

### **6. Conclusions**

Autonomous, air-deployable ambient noise sensor (ANS) drifters have been developed by the Tactical Oceanography Warfare Support (TOWS) program office (Selsor, 1993). The high frequency (> 500 Hz) ambient sound data collected by these buoys can be used to quantify present weather conditions. To evaluate the performance of these drifters, co-located passive microwave satellite data, SSM/I data, from DMSP satellites F-10 and F-13, were processed to measure wind speed and detect precipitation. Using 254 comparison data points, from 154 drifter data days, the correlation between acoustic and satellite derived wind speed measurements is 0.91. The satellite wind speed measurements had an offset of +0.8 m/s when compared to the acoustic measurements.

Precipitation detection is one of the promising features of the acoustic sensor. A comparison of rainfall detection by co-located (spatial and temporal) SSM/I images confirmed the acoustic detection of precipitation for 19 of 21 (90.5%) events. The acoustic sensor did not confirm apparent SSM/I detection of light rain/drizzle during high wind speed ( $> 10$  m/s) conditions. Of course, the SSM/I detection of drizzle is speculative, based on cloud liquid water measurements. High wind is known to disrupt the sound production mechanism for the small raindrops typical of drizzle (Nystuen, 1993) and, thus this finding is not unexpected.

## 7. Acknowledgments

This work was funded through the Oceanographer of the Navy's Center for Tactical Oceanographic Warfare Support (TOWS) program office at the Naval Research Laboratory, Code 7406, Stennis Space Center, MS, under the PE 0604218N R1740 drifting buoy project. Metocean Data Systems Ltd. of Dartmouth, Nova Scotia developed and built the AN/WSQ-6 drifters. SSM/I data were provided by the NASA Marshall Space Flight Center's Global Hydrology and Climate Center.

## Appendix. Algorithm for Weather Classification

The algorithm relies on spectral shape differences to identify five categories of sound source: 1) shipping or other contamination, 2) heavy rain, 3) wind with drizzle, 4) wind only, and 5) bubbles present. It is a modification of the algorithm described in Nystuen and Selsor (1997). It is empirical. Most of the time, the sound field is assumed to be generated by "wind only" processes. Various choices of frequencies were tried to identify times when "unusual" intensities were present. These were assumed to be generated by non-wind sources (rain, drizzle, high seas and shipping). There is evidence of regional variation. In particular, drifters deployed in the Eastern North Pacific recorded high frequency sound levels (at 25 kHz) roughly 2 dB lower than drifters from other locations (N. Atlantic, W. N. Pacific, Gulf of Mexico). This result is in agreement with the previous work (Nystuen and Selsor, 1997). One drifter, #26305, deployed northeast of Japan, reported high frequency sound levels fully 8 dB higher than any other drifter. An explanation for this anomaly is not available. Because of regional variations associated with 25 kHz, the modified algorithm described here mostly uses lower frequencies, in particular 20 kHz sound levels rather than 25 kHz.

The algorithm consists of 1) a check for shipping or other low frequency contamination, 2) a check for the high levels at higher frequencies associated with heavy rain, 3) a check for drizzle, 4) a check for the attenuation of higher frequencies associated with the presence of ambient bubbles. If none of the checks is positive, then the sound source is assumed to be "wind only". The spectral slope test of Vagle et al. (1990) is not used. Quantification of wind speed is possible for "wind only", "wind with drizzle" and "wind with bubbles present", although the wind speed algorithm of Vagle et al. (1990) is strictly valid only for the "wind only" situation (for wind speeds of 2-15 m/s in absence of precipitation). Rainfall rate can also be quantified (Nystuen et al., 1993), although the algorithm was developed in a coastal environment and has not been verified in deep ocean situations. Drizzle should not be quantified as the sound source is a function of wind speed, although it can be assumed that the rainfall rate is not high (< 1 mm/hr).

### Step One: Check for excess low frequency sound.

This test is more "aggressive" than the one described in Nystuen and Selsor (1997). In particular, there is a higher probability that shipping noise will not be detected. The philosophy behind this decision is that high sound levels below 1000 Hertz include distance shipping/manmade noise which may not propagate to the drifter location at the higher frequencies used to quantify local weather conditions. In other words, the high frequency sound levels are not affected by distance shipping noise. This is not true for local shipping/noise which can affect a broad band of frequencies. Usually, shipping has higher levels of low frequency sound relative to high frequency, and thus it is assumed that shipping/manmade noise is present when such conditions are detected (Lemon et al., 1984). If excess low frequency sound (at 4 kHz) is present relative to high frequency (at 20 kHz), then the likelihood of contamination at 8 kHz, where the acoustic wind speed algorithm is applied, is very high. The test is shown in Fig. A1 and uses 4000 and 20000 Hertz.

If

$$\text{SPL}_{20000} < 0.7 \cdot \text{SPL}_{4000} + 2$$

and

$$\text{SPL}_{20000} < (-0.7) \cdot \text{SPL}_{4000} + 86$$

then shipping (or other) contamination is suspected.  $SPL_x$  is the sound pressure level in dB relative to  $1 \mu\text{Pa}^2/\text{Hz}$  at frequency  $x$ . The data point should not be further processed.

Step Two: Check for high frequency sound associated with heavy rain.

Heavy rain produces extremely high sound intensities at all frequencies (above 500 Hertz), especially above 20 kHz. The test (Fig. A2) checks for high sound levels at 20 kHz relative to 5 kHz. The vertical line separating rain ( $SPL_{5000} > 52 \text{ dB}$ ) from drizzle ( $SPL_{5000} < 52 \text{ dB}$ ) is present because the rainfall rate algorithm of Nystuen et al. (1993) is valid only for sound levels above 52 dB. Bubbles present during heavy rain can depress the sound levels at 20 kHz so much that the test shown in Fig. A2 does not detect the rain. A second rainfall test is used (Fig. A3) to detect heavy rain when ambient bubbles are present. This is a relatively "aggressive" test and may falsely detect rainfall when, in fact, high bubble populations are present due just to extensive wave breaking. Further research into the identification of sound from rain in the present of high wind (bubbles present) is needed.

Test 1: If

$$SPL_{20000} > 47.5 \quad \text{or} \quad SPL_{20000} > 0.5 \cdot SPL_{5000} + 19$$

and

$$SPL_{5000} > 52 \text{ dB}$$

or

Test 2: If

$$SPL_{20000} + 1.1 \cdot SPL_{8000} > 109.5$$

then heavy rain is detected. The rainfall rate algorithm of Nystuen et al. (1993) can be applied to the data point. This algorithm is given by

$$\log_{10} R = \frac{SPL_{5000} - 51.9}{10.6}$$

where  $R$  is rainfall rate in mm/hr. No further processing of the data is possible. The sound from heavy rain obscures the sound generated by other processes, in particular, wind associated sound.

Step Three: Check for drizzle.

Very light rain is observed to increase the sound levels from 13-20 kHz due to the physical mechanism for sound production by small (1 mm diameter) raindrops. If only small raindrops are present (drizzle), then the lower frequencies (below 13 kHz) should not be affected by the drizzle. Therefore, in theory, the wind speed measurement in the presence of drizzle is good. However, as drizzle turns to rain, the sound level at 8 kHz, where the acoustic wind speed algorithm is applied, will become contaminated by rain noise. Thus, wind speed calculated when drizzle is present should be flagged as less accurate (by over-estimation) than the "wind only" category. The drizzle test is shown in Fig. A3 using 8000 and 20000 Hertz.

If

$$SPL_{20000} > 0.8 \cdot SPL_{8000} + 4 \quad \text{and} \quad SPL_{20000} > 36 \text{ dB}$$

then drizzle is present. The data can be further processed to measure wind speed, but a "drizzle" flag should be attached to the wind speed estimate. Quantification of rainfall rate should not be

attempted as the small drop sound production mechanism is sensitive to wind (Nystuen, 1993). A rainfall rate of 1 mm/hr is proposed as a generic "light" rainfall rate.

Step Four: Check for "bubbles present".

When high populations of ambient bubbles are present in the upper part of the ocean surface layer, the shape of the sound spectrum is modified. This is assumed to be due to breaking waves from high winds (Farmer and Lemon, 1984) or changing wind/wave sea conditions (Nystuen and Farmer, 1989). The high frequency sound intensities are attenuated as small bubbles responsible for this attenuation are present in the water. Lower frequencies (5000 Hertz and lower) are not affected as the bubbles required to attenuate the lower frequencies are too buoyant to remain in the water. Thus, it is thought that the lower frequencies continue to reflect increased breaking, and can still be used to measure wind speed. Note, however, that the Vagle et al. wind speed algorithm was developed using data for wind speeds up to 15 m/s and may not be accurate above 15 m/s. The test for "bubbles present" uses 5000 and 25000 Hertz and is shown in Fig. A4.

If

$$SPL_{5000} > 58 \quad \text{and} \quad SPL_{25000} < 44.5$$

then ambient bubbles are detected. The Vagle et al. wind speed algorithm can be applied, however a "high seas" flag should be attached.

Step Five: Apply the Vagle et al. (1990) wind speed algorithm. If shipping or heavy rain "contamination" is detected, the acoustical wind speed measurement is not valid and should not be attempted. If drizzle or high seas are detected, then the wind speed algorithm can be applied, but with caution (the points should be flagged). Otherwise, the wind speed algorithm can be applied. It is valid for wind speeds from 2-15 m/s  $\pm$  2 m/s. Under 2 m/s, no wave (no wavelet) breaking occurs and thus there is no mechanism for wind to produce sound underwater. The algorithm was developed using wind speeds less than 15 m/s. While it may still be valid above 15 m/s, there is no verification of such performance and thus the error is unknown.

The Vagle et al. (1990) wind speed algorithm is given by:

$$U_{10} = \frac{10^{SPL_{5000}/20} + 104.5}{53.91}$$

where  $U_{10}$  is the 10-meter wind speed in m/s.

## References:

- Barrett, E.C., J. Dodge, H.M. Goodman, J. Janowiak, C. Kidd and E.A. Smith, 1994: The first WetNet precipitation intercomparison project (PIP-1). *Remote Sensing Reviews* **11**, 49-60.
- Dailey, C.H., 1991: Analysis of wind and rainfall measurements from acoustic drifters. M.S. thesis, Dept. of Oceanography, Naval Postgraduate School, Monterey, CA 93943, 109 pp.  
[Available from Superintendent, Code 043, Naval Postgraduate School, Monterey, CA 93943-5000 via the Defense Technical Information Center, Cameron Station, Alexandria, VA 22304-6145.]
- Farmer, D.M. and D.D. Lemon, 1984: The influence of bubbles on ambient noise in the ocean at high wind speeds. *J. Phys. Ocean.* **14**, 1762-1778.
- Ferraro, R.R., F. Weng, N.C. Grody and A. Basist, 1996. An eight-year (1987-1994) time series of rainfall, clouds, water vapor, snow cover, and sea ice derived from SSM/I measurements. *Bull. Am. Meteor. Soc.* **77**, 891-905.
- Goodberlet, M.A., C.T. Swift, and J.C. Wilkerson, 1989: Remote sensing of ocean surface winds with the special sensor microwave/imager. *J. Geophys. Res.* **94**, 14547-14555.
- Lemon, D.D., D.M. Farmer and D.R. Watts, 1984: Acoustic measurements of wind speed and precipitation over a continental shelf. *J. Geophys. Res.* **89**, 3462-3472.
- McCormick, M.J., R.L. Pickett and G.S. Miller, 1990: A field evaluation of new satellite-tracked buoys: A LORAN-C position recording and a sonobuoy type drifter. *MTS Journal* **25**, 29-33.
- Medwin, H. and M.M. Beaky, 1989: Bubble sources of the Knudsen sea noise spectra. *J. Acoust. Soc. Am.* **86**, 1124-1130.
- Medwin, H., J.A. Nystuen, P.W. Jacobus, D.E. Snyder and L.H. Ostwald, 1992: The anatomy of underwater rain noise. *J. Acoust. Soc. Am.* **92**, 1613-1623.
- Nystuen, J.A., 1993: An Explanation of the Sound Generated by Light Rain in the Presence of Wind. *Natural Physical Sources of Underwater Sound*, B.R. Kerman, Ed., Kluwer Academic Publishers, 659-668.
- Nystuen, J.A., 1996: Acoustical Rainfall Analysis: Rainfall drop size distribution using the underwater sound field. *J. Atmos. and Ocean. Tech.* **13**, 74-84.
- Nystuen, J.A., C.C. McGlothin and M.S. Cook, 1993: The underwater sound generated by heavy precipitation. *J. Acoust. Soc. Am.* **93**, 3169-3177.
- Nystuen, J.A. and D.M. Farmer, 1989: Precipitation in the Canadian Atlantic Storms Program: Measurements of the Acoustic Signature. *Atmos. Ocean* **27**, 237-257.
- Nystuen, J.A., and H.D. Selsor, 1997: Weather classification using passive acoustic drifters. *J. Atmos. Oceanic Tech.* **14**, 656-666.

- Pumphrey, H.C., L.A. Crum and L. Bjorno, 1989: Underwater sound produced by individual drop impacts and rainfall. *J. Acoust. Soc. Am.* **85**, 1518-1526.
- Selsor, H.D., 1993: Data from the sea: Navy Drifting Buoy Program. *Sea Technology* **34**, 53-58.
- Stewart, R.H., 1985: *Methods of Satellite Oceanography*. University of California Press, 360 pp.
- Vagle, S., W.G. Large and D.M. Farmer, 1990: An evaluation of the WOTAN technique for inferring oceanic winds from underwater sound. *J. Atmos. and Oceanic Tech.* **7**, 576-595.
- Weng, F. and N.C. Grody, 1994: Retrieval of cloud liquid water using the special sensor microwave imager (SSM/I). *J. Geophys. Res.* **99**, 25535-25551.
- Wentz, F., 1994: User's manual SSM/I-2 geophysical tapes. 20 pp. [Available from Remote Sensing Systems, 1101 College Ave. Suite 220, Santa Rosa, CA 95404]
- Wenz, G.M., 1962: Acoustic ambient noise in the oceans: Spectra and sources. *J. Acoust. Soc. Am.* **34**, 1936-1956.
- Wilheit, T.T., A.T.C. Chang and L.S. Chiu, 1991: Retrieval of monthly rainfall indices from microwave radiometric measurements using probability distribution functions. *J. Atmos. Oceanic Tech.* **8**, 118-136.

## List of Figures:

Figure 1. Physical configuration of a deployed ANS drifter.

Figure 2. Selected sound spectra from ANS Drifter #14270. Several "wind only" spectra are shown: background (calm conditions); 4 m/s (wind increasing); 7 m/s (wind increasing); 10 m/s (wind decreasing) and 17 m/s (hydrophone broke soon afterwards). The 17 m/s spectra shows the steepened higher frequency spectral slope associated with ambient bubble in the ocean surface layer. Three rainfall detections are shown: r1, a light drizzle showing the characteristic spectral peak associated with small raindrops, r2 a "light rain" detection with an acoustic rainfall rate of 1.4 mm/hr; the microwave satellite estimate is 2 mm/hr, and r3, a heavy rain during rapidly rising wind conditions. The acoustic rainfall rate is 7.7 mm/hr; the microwave satellite rainfall rate is 3 mm/hr. For r2 and r3, no "peak" is evident in the sound spectrum, however relatively more high frequency energy is present allowing acoustic detection of rain.

Figure 3. Weather classification for ANS Drifter #26307. By comparing the sound level at 5 kHz with the sound level at 25 kHz, clustering of data points allows weather classification (Nystuen and Selsor, 1997). Wind only (•) data points usually form a well-defined locus of points. Drizzle (⊕) and rain (⊗) generate relatively more high frequency sound, while shipping (×) has relatively more low frequency components. Bubbles present (+) is identified by reduced levels at 25 kHz together with very high levels at 5 kHz.

Figure 4. An alternative classification comparison is shown for Drifter #14270. The high frequency (8-25 kHz) spectral slope can also be used to detect precipitation. One "drizzle" event (JD 92.5), two "light rains" in moderate wind conditions (JD 97.6 and JD 101.8), and one "heavy rain" in high wind conditions (JD 102.6) are detected.

Figure 5. Drifter tracks for Drifters #14269, #14270 and #14272. The first and last days (Julian date) of valid acoustical data are labeled for each drifter.

Figure 6. Atmospheric pressure, temperature and sea surface temperature for Drifters #14269 (dash-dot line), #14270 (dashed) and #14272 (solid). Similar conditions are detected by each drifter.

Figure 7. Acoustic (solid line) and satellite (+) wind speed comparisons temperature for Drifters #14269, #14270 and #14272.

Figure 8. Acoustic (\*) and satellite (o) precipitation (drizzle and rain) detections for Drifters #14269, #14270 and #14272.

Figure 9. Drifter tracks for ANS Drifters #26304, #26305, #26306 and #26307.

Figure 10. Atmospheric pressure, temperature and sea surface temperature for ANS Drifters #26304 (solid line) and #26305 (dashed line).

Figure 11. Acoustic (solid line) and satellite (+) wind speed comparisons temperature for Drifters #26304 and #26305.

Figure 12. Acoustic (\*) and satellite (o) precipitation (drizzle and rain) detections for Drifter #26304.

Figure 13. Comparison of 5 and 25 kHz sound levels for Drifters #26304 (+), #26305 (o), #26306 (x) and #26307 (\*). The 25 kHz sound levels for Drifter #26305 are 8 decibels higher than the levels reported by the other buoys. This difference does not appear to affect the acoustic wind speed estimates, which use the sound levels at 8 kHz.

Figure 14. Sound levels for Drifter #26305. Near the end of the deployment at JD 81.3, the sound levels at all frequencies from 5 Hz to 25 kHz, increased sharply. This anomaly is probably manmade noise as few natural sound sources span such a wide range of frequencies.

Figure 15. Atmospheric pressure, temperature and sea surface temperature for ANS Drifters #26306 (dashed line) and #26307 (solid line).

Figure 16. Acoustic (solid line) and satellite (+) wind speed comparisons for Drifters #26306 and #26307.

Figure 17. Acoustic (\*) and satellite (o) precipitation (drizzle and rain) detections for Drifters #26306 and #26307.

Figure 18. Two acoustic rain detections (\*) missed by the SSM/I sensors. Acoustic (+) and satellite (o) wind speed data are also shown.

Figure 19. Sound spectra for Drifter #14268. These spectra show the characteristic shape of sound generated by snapping shrimp. This buoy was grounded on a coral reef.

Figure 20. Wind speed and rainfall rate comparisons for Drifter #14275. Acoustic (+) and satellite (o) wind speed measurements are in the upper panel. The acoustic rain (\*) and satellite drizzle (o) detections are shown in the lower panel.

Figure 21. Environmental data for Drifter #26308. The acoustic (+) and satellite (o) wind speed measurements are shown in the upper panel. The sea surface temperature (SST) and air temperature are shown in the lower panel.

Figure 22. Comparison of ANS and SSM/I wind speed measurements. Data from the eastern North Pacific (x), warm water drifters (\*), the western North Pacific (+) and north of Scotland (o) show no regional or environmental trends.

Figure A1. Shipping detection test using 4000 and 20000 Hz. Data from ANS drifters deployed in the eastern North Pacific (+), warm water (x), western North Pacific (o) and north of Scotland (\*) are shown.

Figure A2. Rain detection test (Test #1) using 5000 and 20000 Hz. Data from ANS drifters deployed in the eastern North Pacific (+), warm water (x), western North Pacific (o) and north of Scotland (\*) are shown.

Figure A3. Rain (Test #2) and drizzle detection test using 8000 and 20000 Hz. Data from ANS drifters deployed in the eastern North Pacific (+), warm water (x), western North Pacific (o) and north of Scotland (\*) are shown. This combination of frequencies showed the least amount of regional variations in sound levels.

Figure A4. Bubble present test using 5000 and 25000 Hz. Data from ANS drifters deployed in the eastern North Pacific (+), warm water (x), western North Pacific (o) and north of Scotland (\*) are shown.

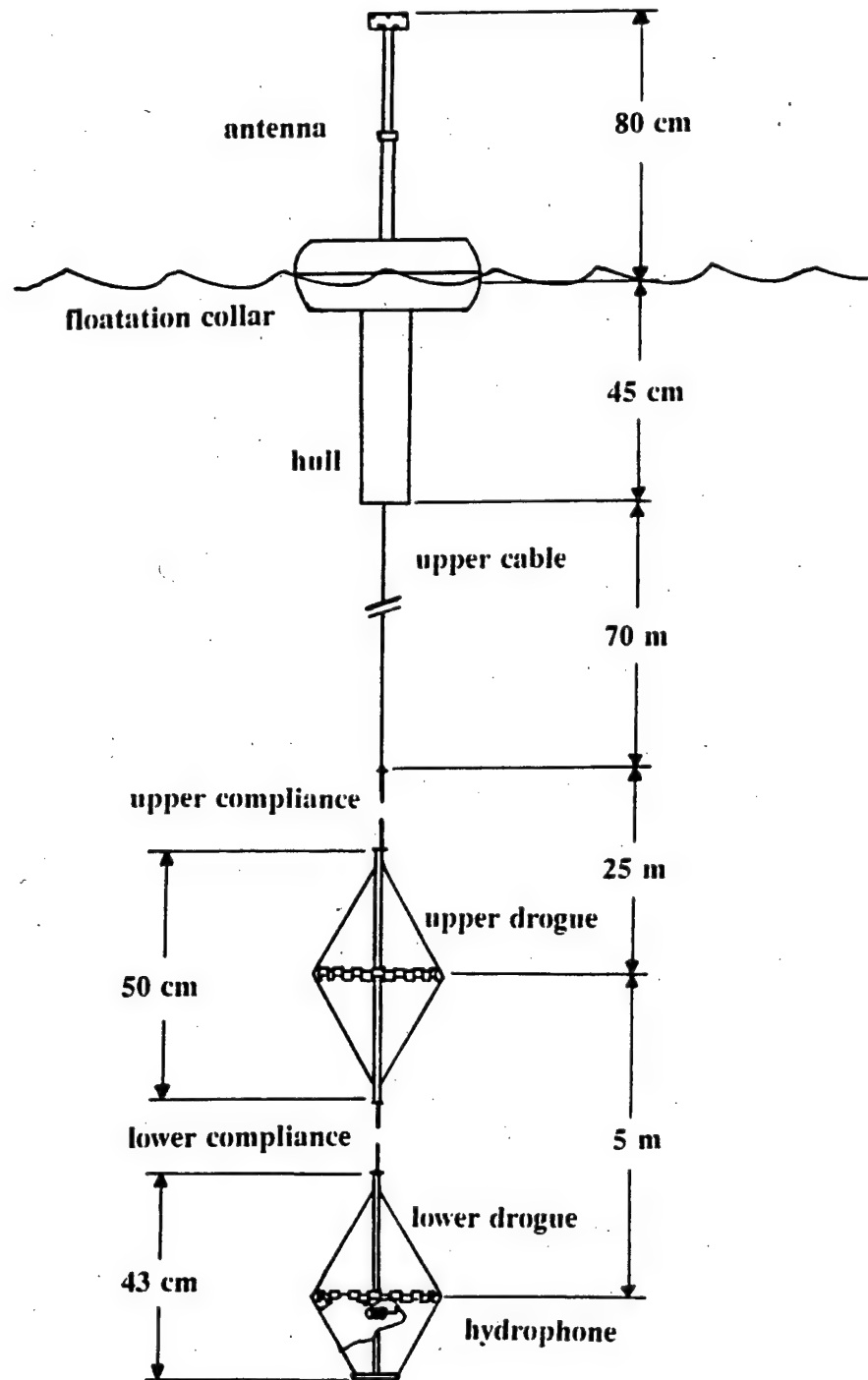
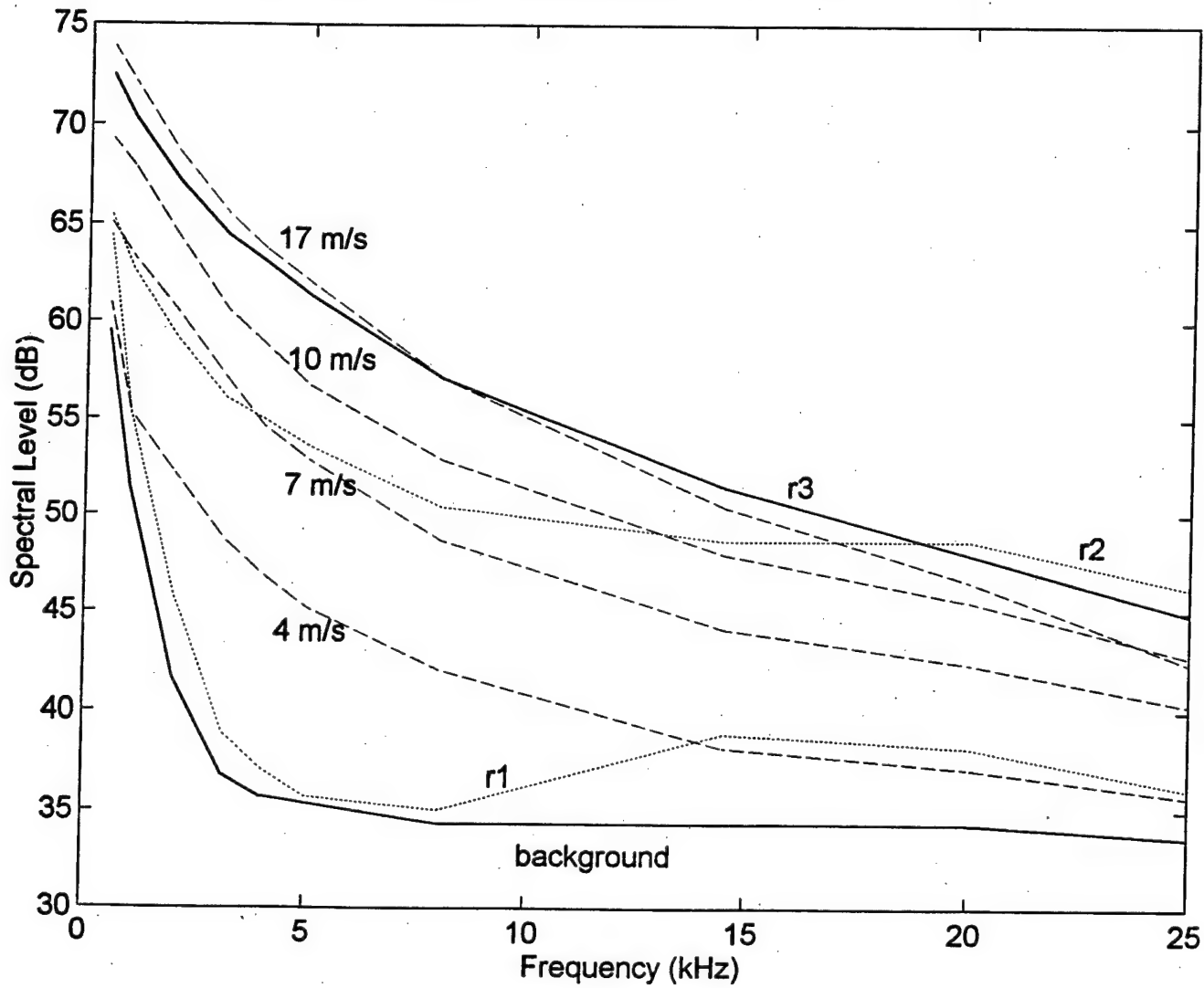


Figure 1. Physical configuration of a deployed ANS drifter.

Figure 2. Selected sound spectra from ANS Drifter #14270. Several "wind only" spectra are shown: background (calm conditions); 4 m/s (wind increasing); 7 m/s (wind increasing); 10 m/s (wind decreasing) and 17 m/s (hydrophone broke soon afterwards). The 17 m/s spectra shows the steepened higher frequency spectral slope associated with ambient bubble in the ocean surface layer. Three rainfall detections are shown: r1, a light drizzle showing the characteristic spectral peak associated with small raindrops, r2 a "light rain" detection with an acoustic rainfall rate of 1.4 mm/hr; the microwave satellite estimate is 2 mm/hr, and r3, a heavy rain during rapidly rising wind conditions. The acoustic rainfall rate is 7.7 mm/hr; the microwave satellite rainfall rate is 3 mm/hr. For r2 and r3, no "peak" is evident in the sound spectrum, however relatively more high frequency energy is present allowing acoustic detection of rain.



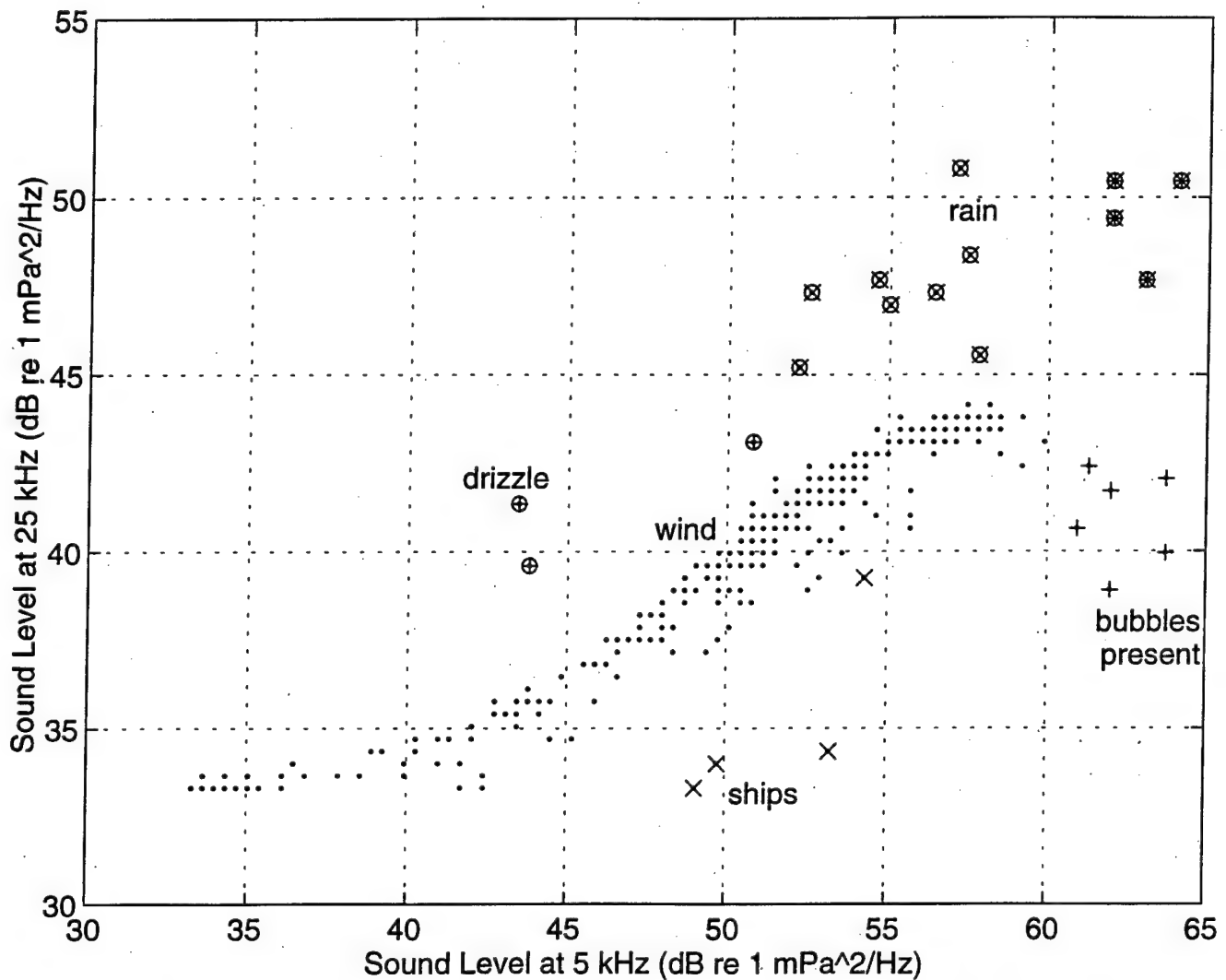


Figure 3. Weather classification for ANS Drifter #26307. By comparing the sound level at 5 kHz with the sound level at 25 kHz, clustering of data points allows weather classification (Nystuen and Selsor, 1997). Wind only ( $\bullet$ ) data points usually form a well-defined locus of points. Drizzle ( $\oplus$ ) and rain ( $\otimes$ ) generate relatively more high frequency sound, while shipping ( $\times$ ) has relatively more low frequency components. Bubbles present (+) is identified by reduced levels at 25 kHz together with very high levels at 5 kHz.

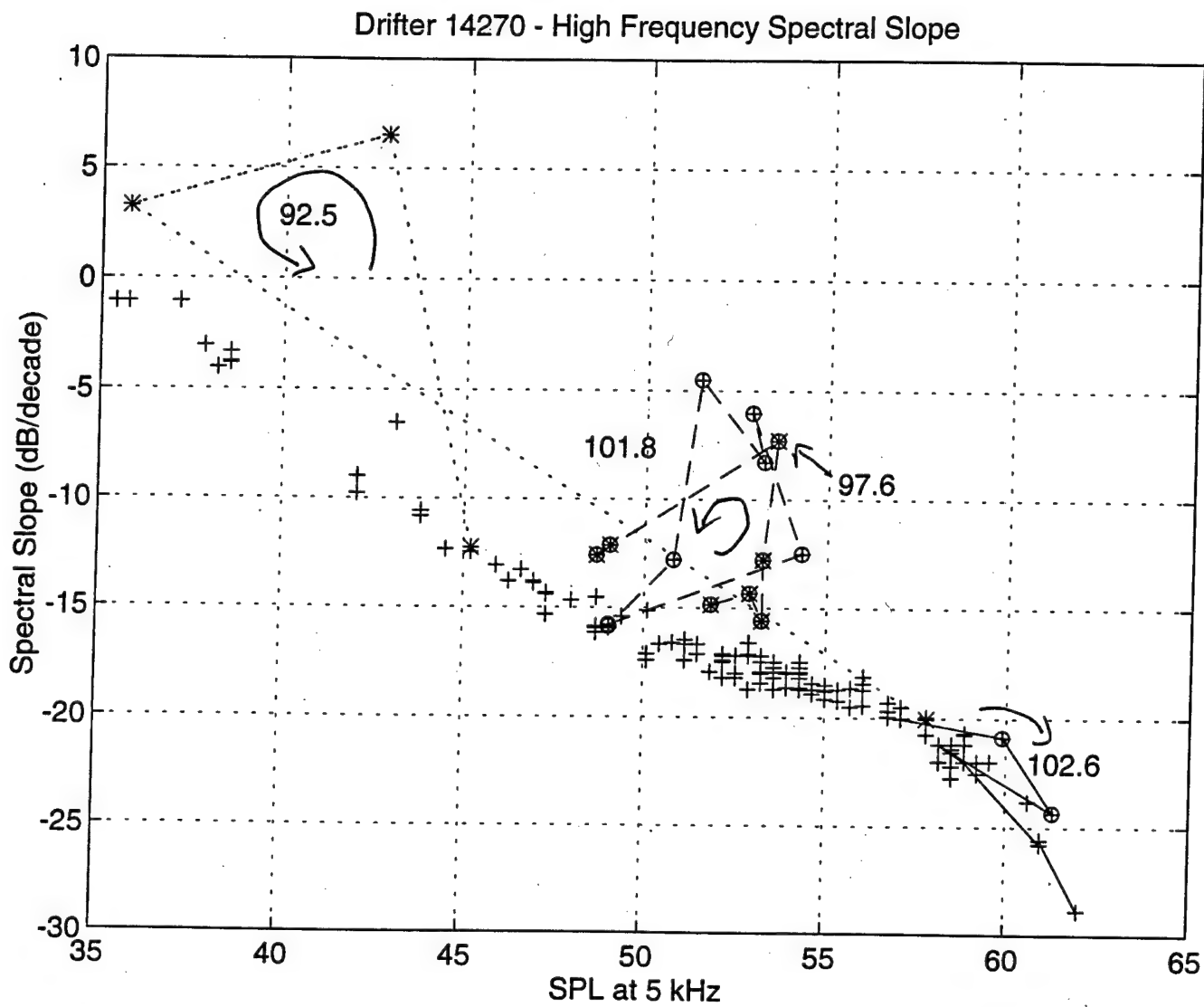


Figure 4. An alternative classification comparison is shown for Drifter #14270. The high frequency (8-25 kHz) spectral slope can also be used to detect precipitation. One "drizzle" event (JD 92.5), two "light rains" in moderate wind conditions (JD 97.6 and JD 101.8), and one "heavy rain" in high wind conditions (JD 102.6) are detected.

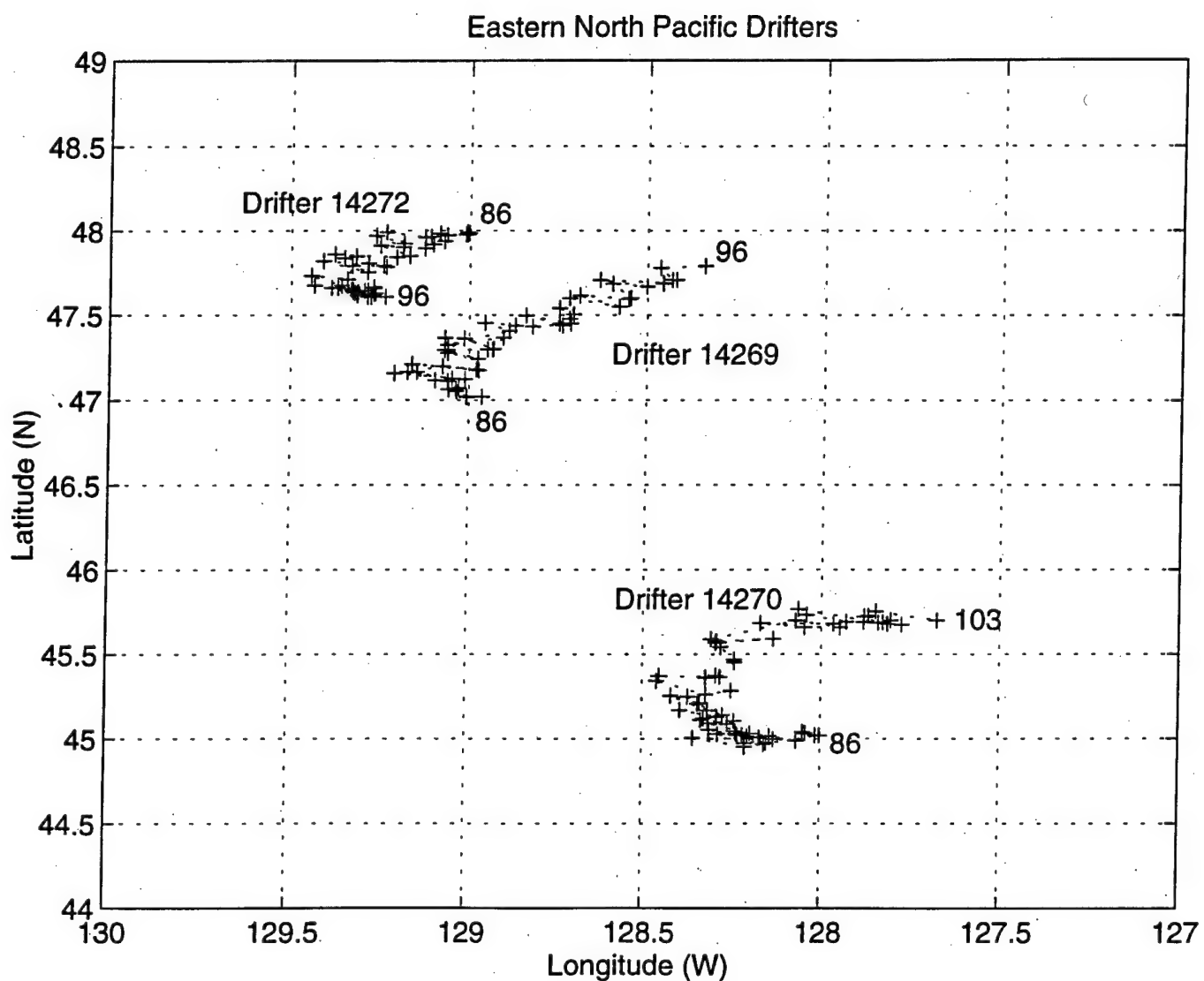


Figure 5. Drifter tracks for Drifters #14269, #14270 and #14272. The first and last days (Julian date) of valid acoustical data are labeled for each drifter.

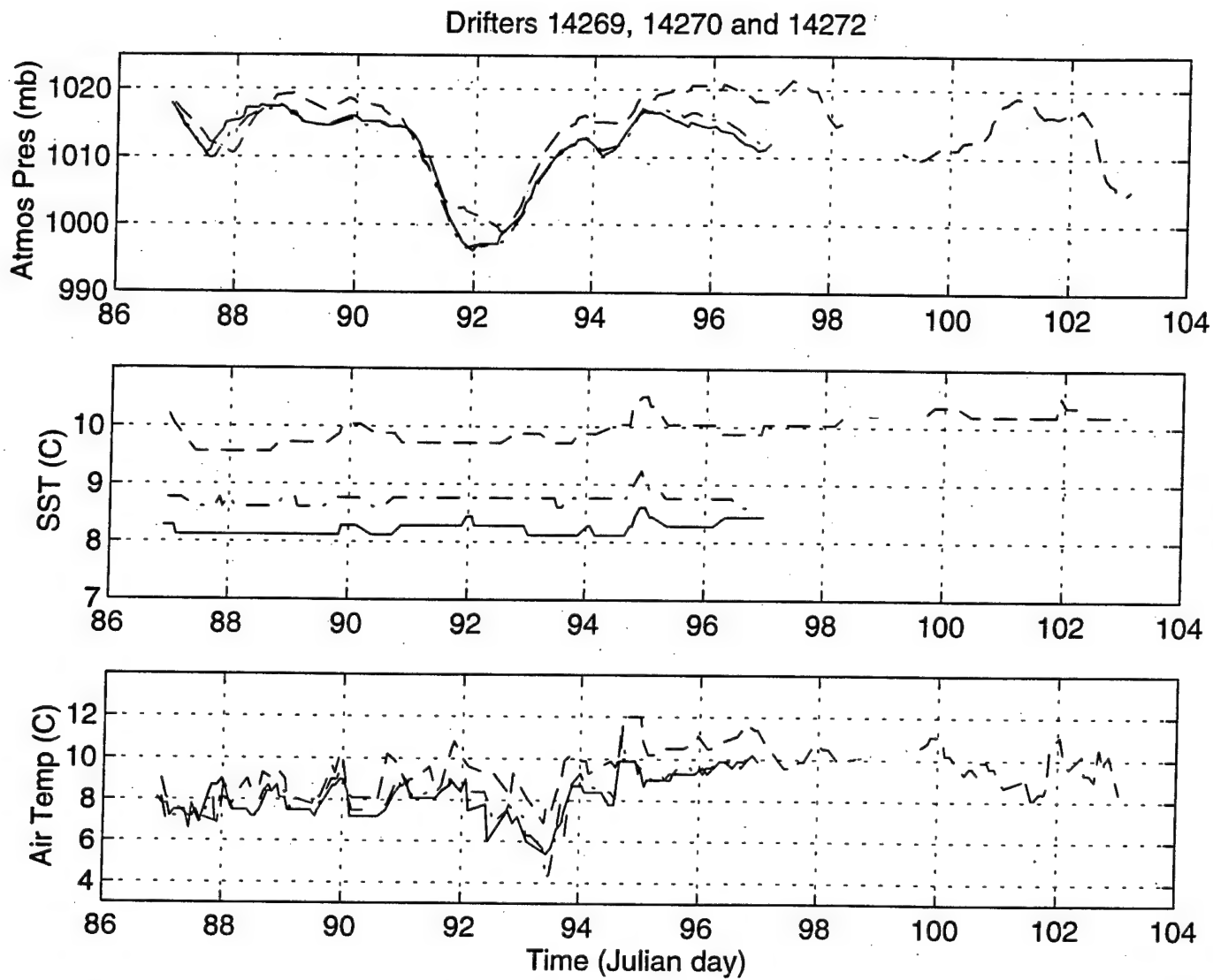


Figure 6. Atmospheric pressure, temperature and sea surface temperature for Drifters #14269 (dash-dot line), #14270 (dashed) and #14272 (solid). Similar conditions are detected by each drifter.

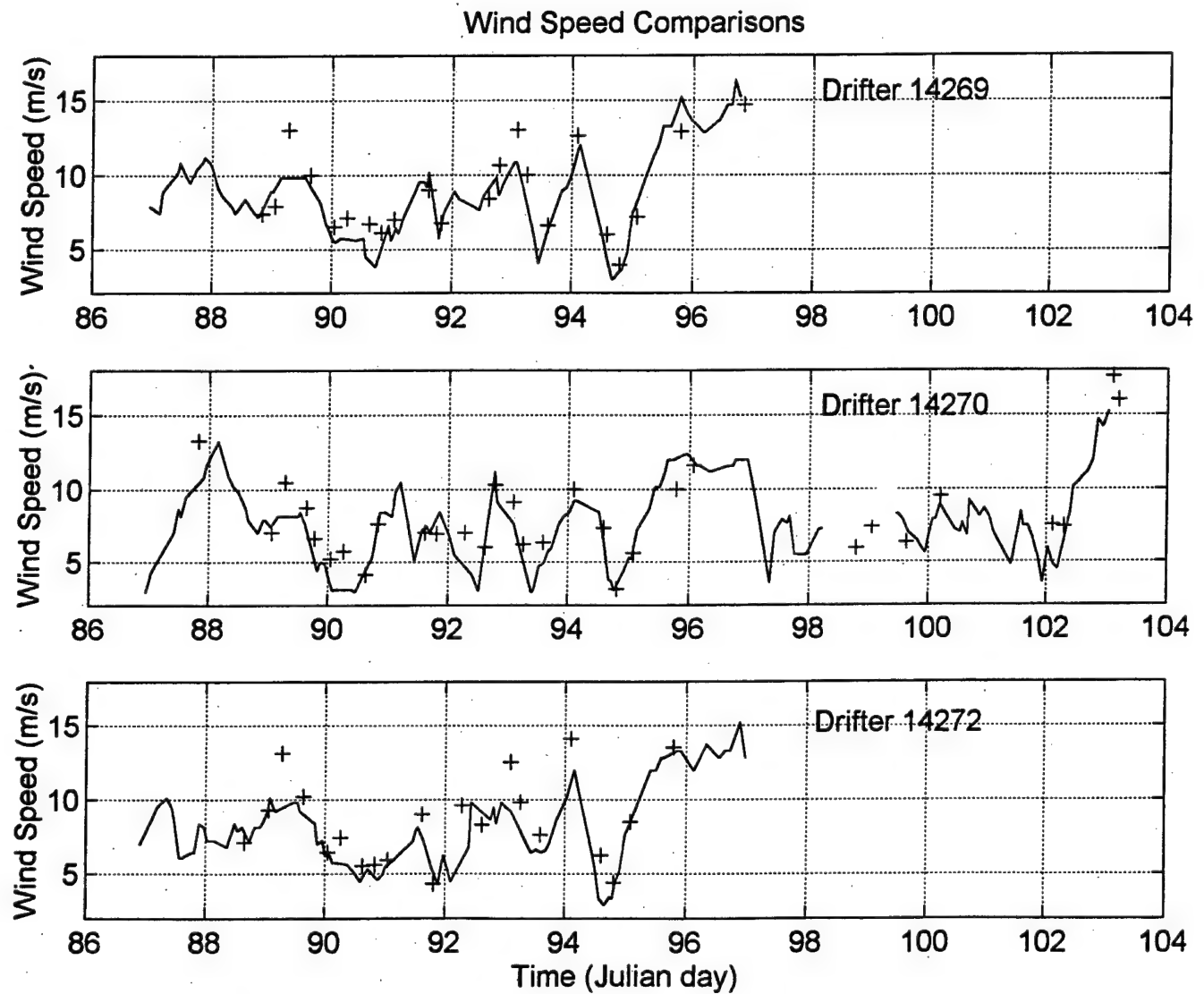


Figure 7. Acoustic (solid line) and satellite (+) wind speed comparisons temperature for Drifters #14269, #14270 and #14272.

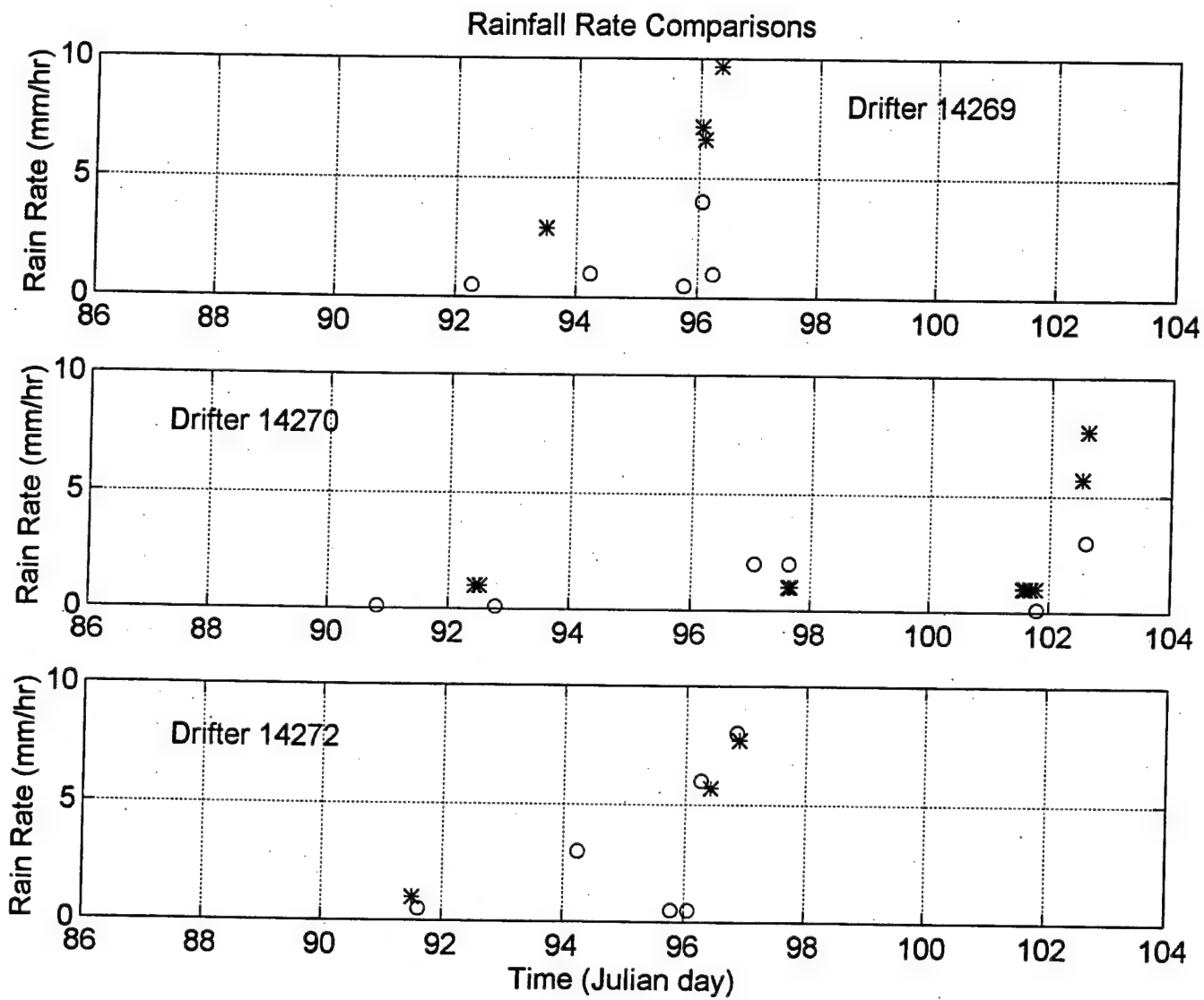


Figure 8. Acoustic (\*) and satellite (o) precipitation (drizzle and rain) detections for Drifters #14269, #14270 and #14272.

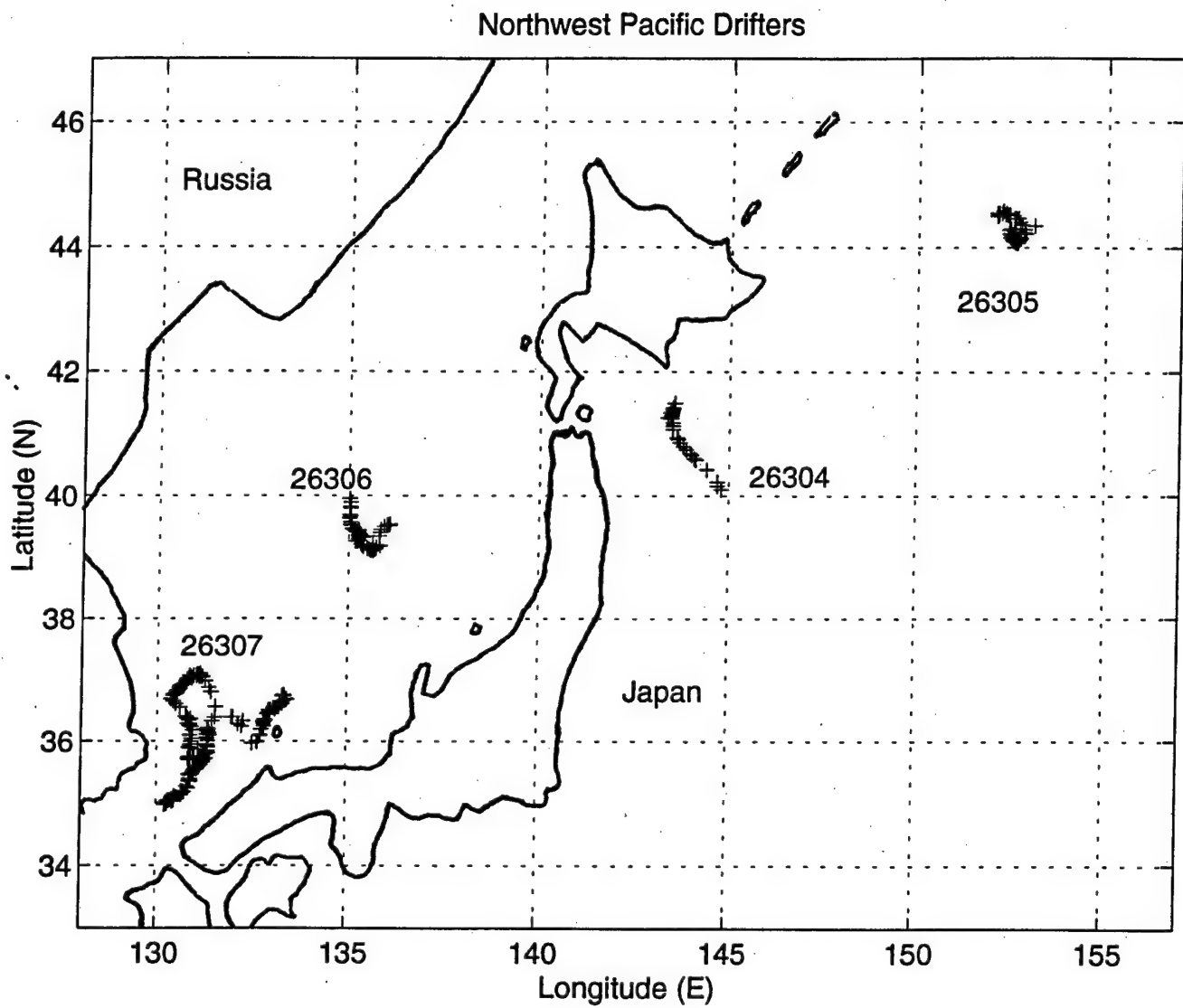


Figure 9. Drifter tracks for ANS Drifters #26304, #26305, #26306 and #26307.

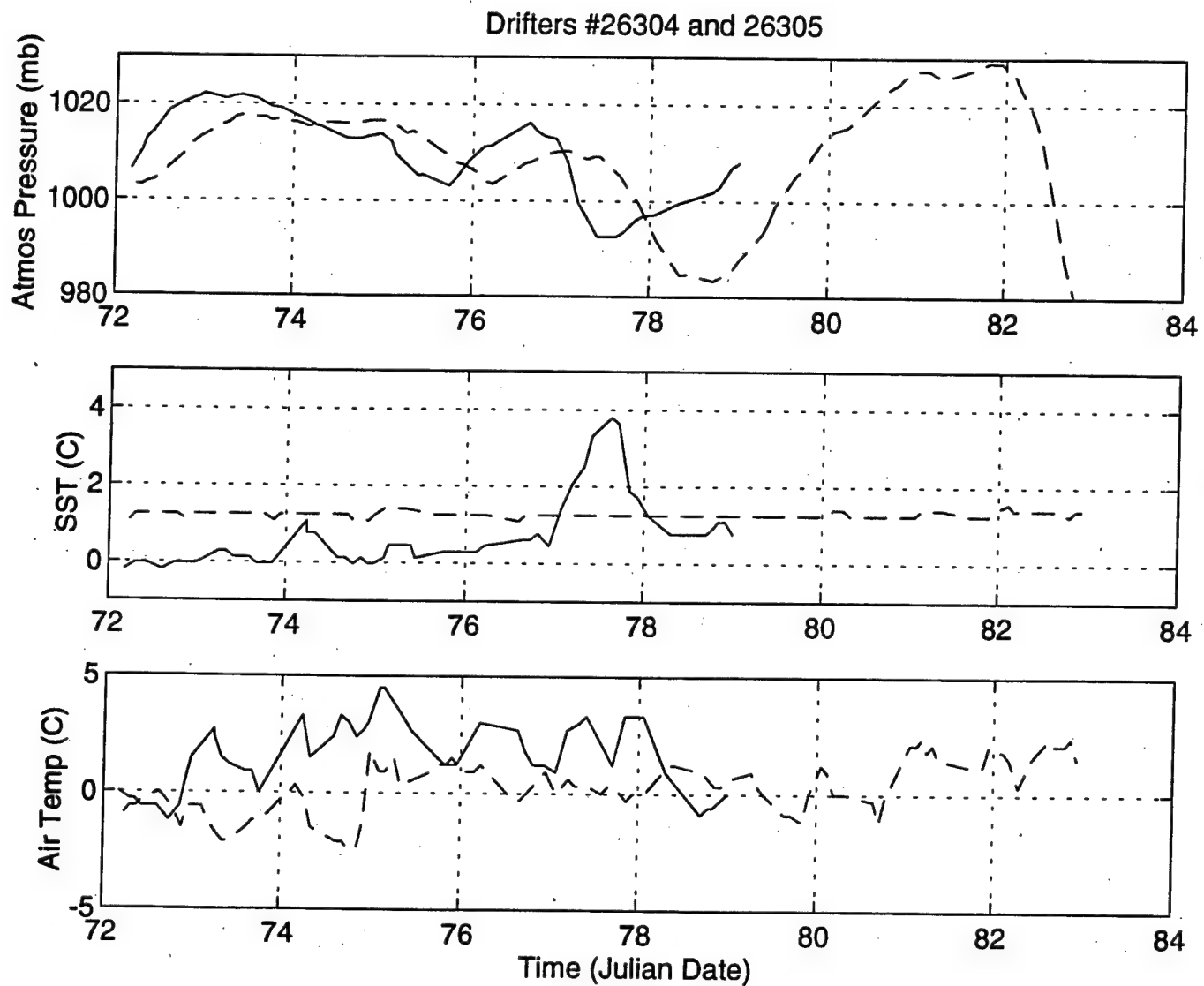
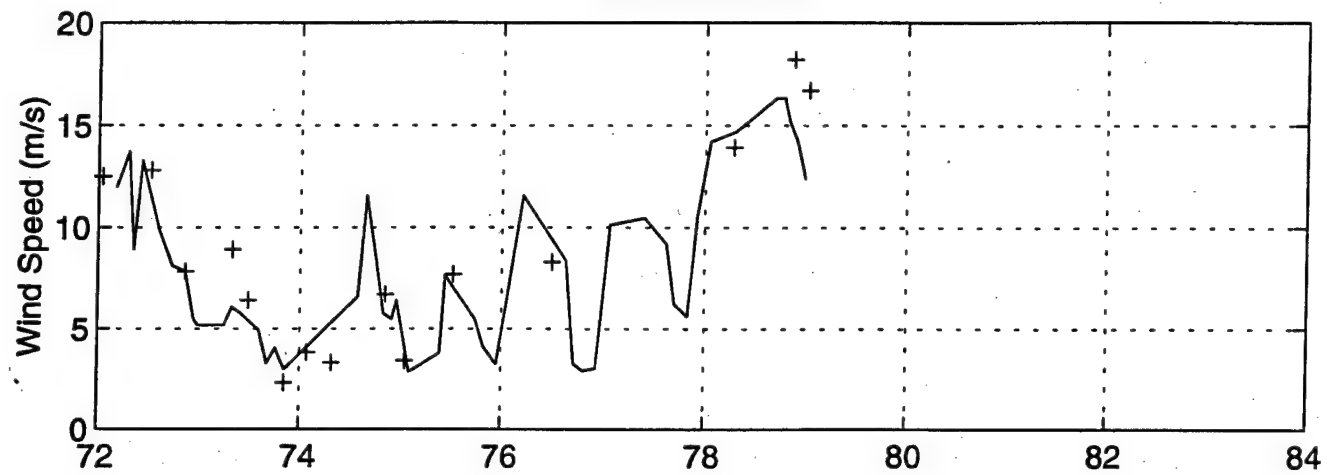


Figure 10. Atmospheric pressure, temperature and sea surface temperature for ANS Drifters #26304 (solid line) and #26305 (dashed line).

Drifter #26304



Drifter #26305

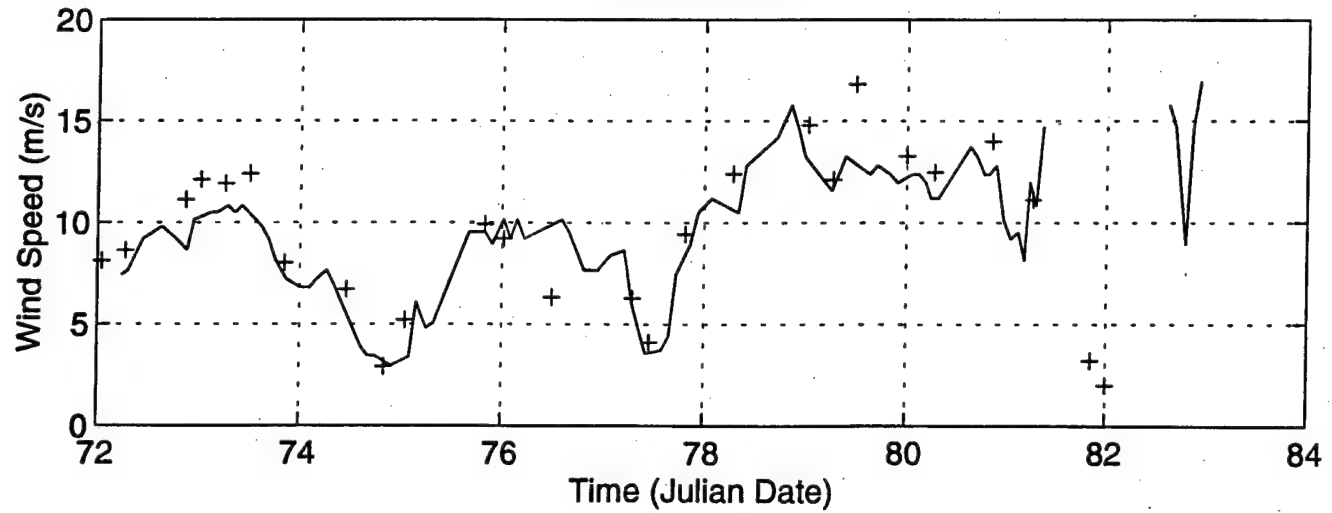


Figure 11. Acoustic (solid line) and satellite (+) wind speed comparisons temperature for Drifters #26304 and #26305.

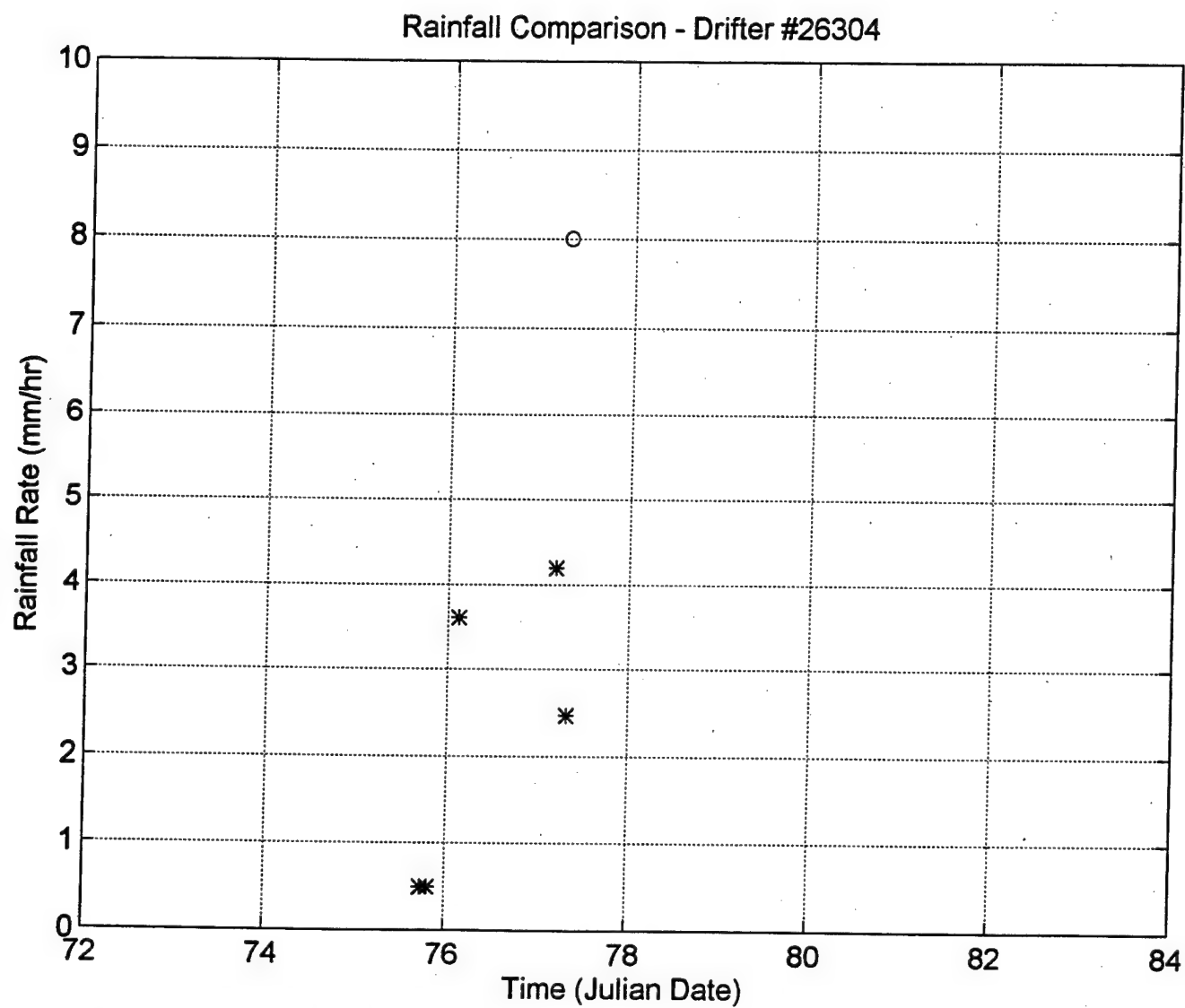


Figure 12. Acoustic (\*) and satellite (o) precipitation (drizzle and rain) detections for Drifter #26304.

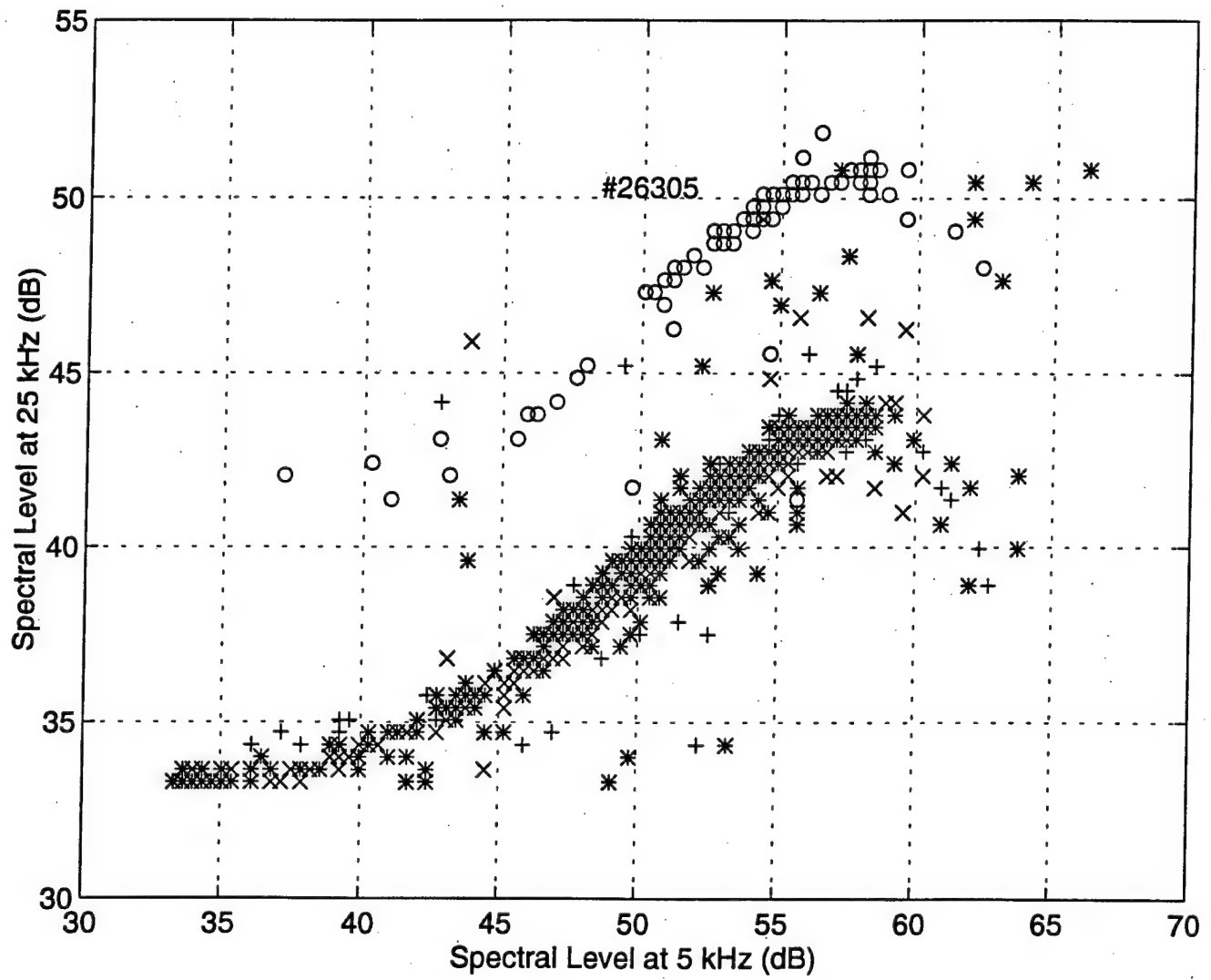


Figure 13. Comparison of 5 and 25 kHz sound levels for Drifters #26304 (+), #26305 (o), #26306 (x) and #26307 (\*). The 25 kHz sound levels for Drifter #26305 are 8 decibels higher than the levels reported by the other buoys. This difference does not appear to affect the acoustic wind speed estimates, which use the sound levels at 8 kHz.

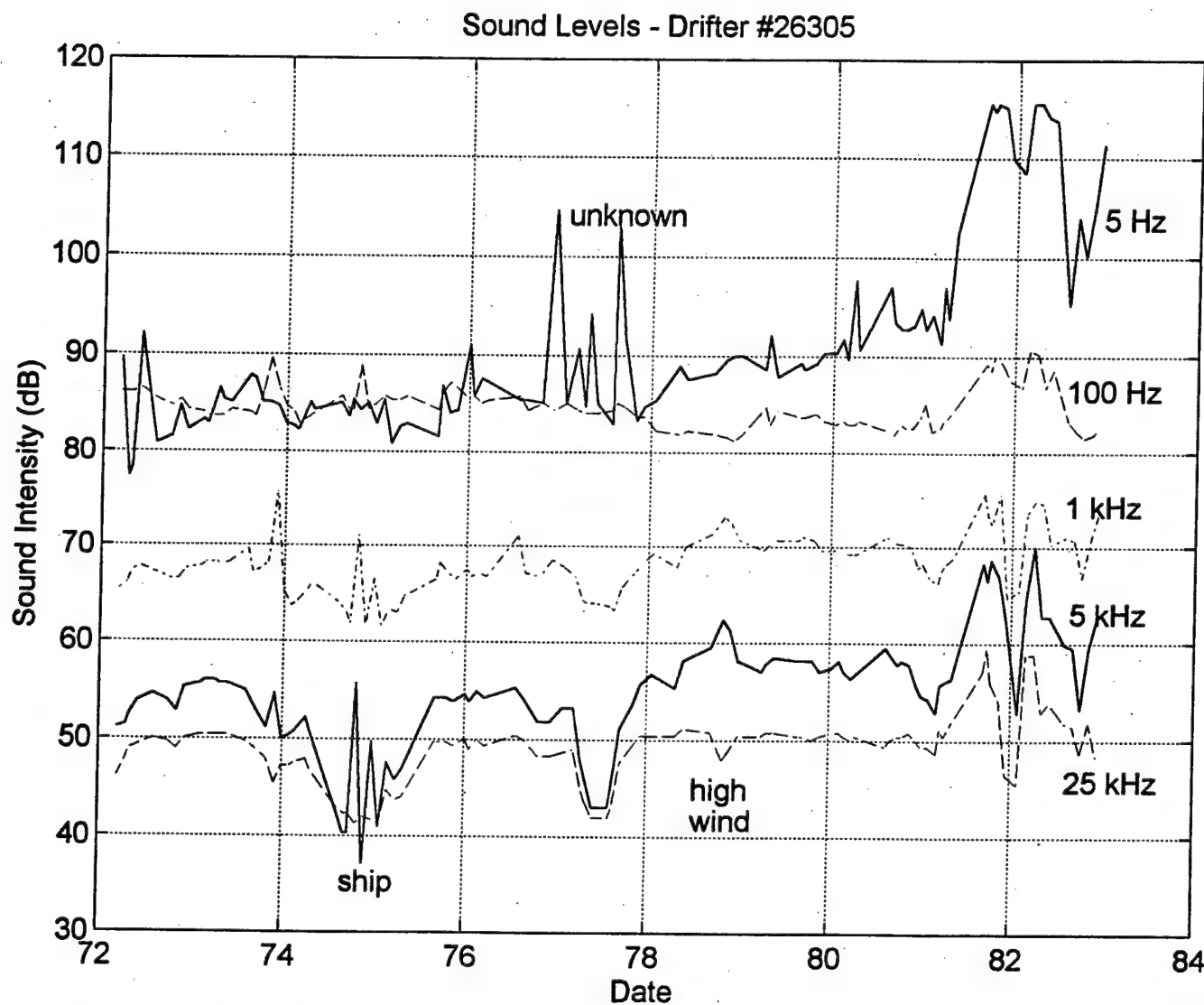


Figure 14. Sound levels for Drifter #26305. Near the end of the deployment at JD 81.3, the sound levels at all frequencies from 5 Hz to 25 kHz, increased sharply. This anomaly is probably manmade noise as few natural sound sources span such a wide range of frequencies.

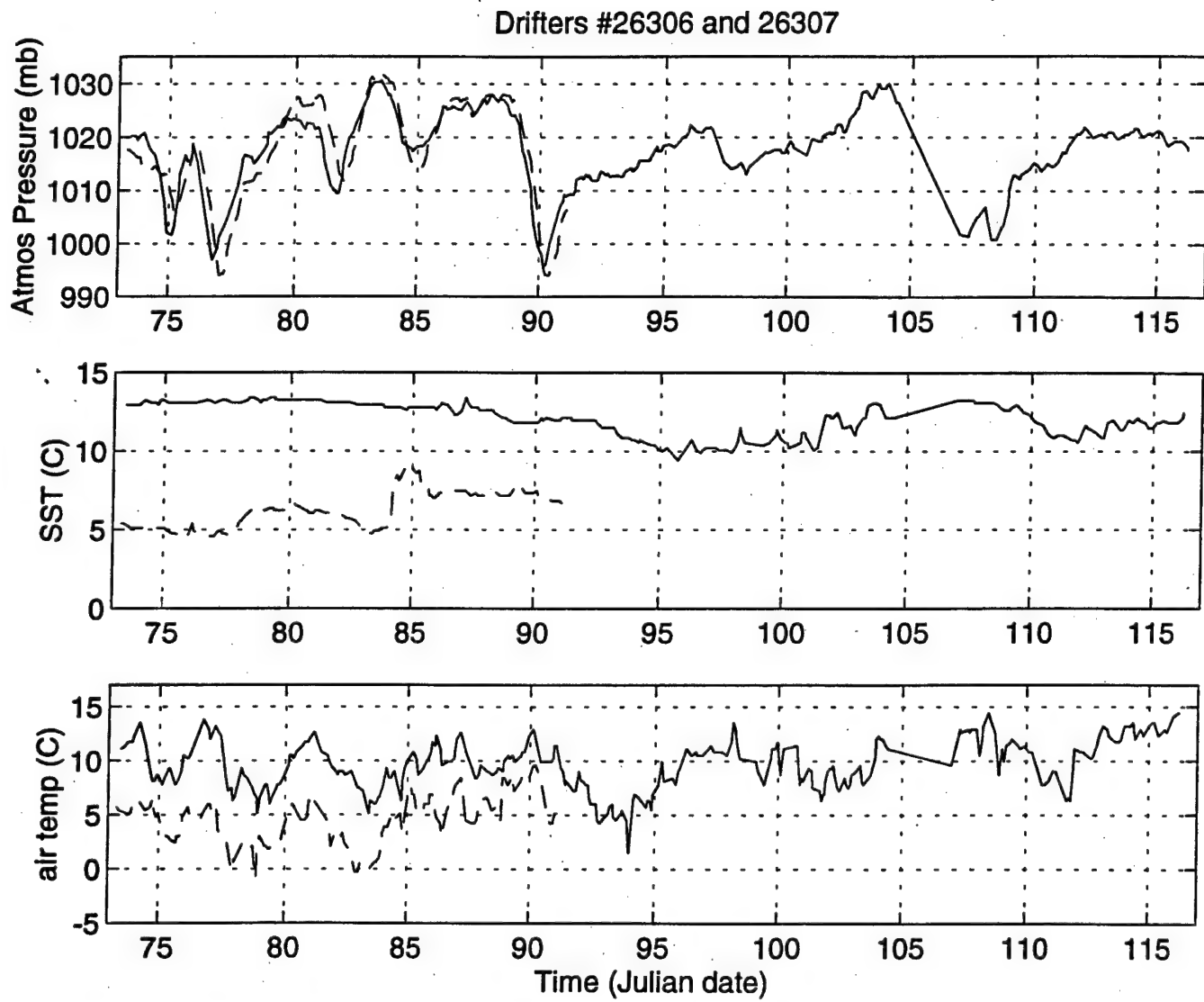
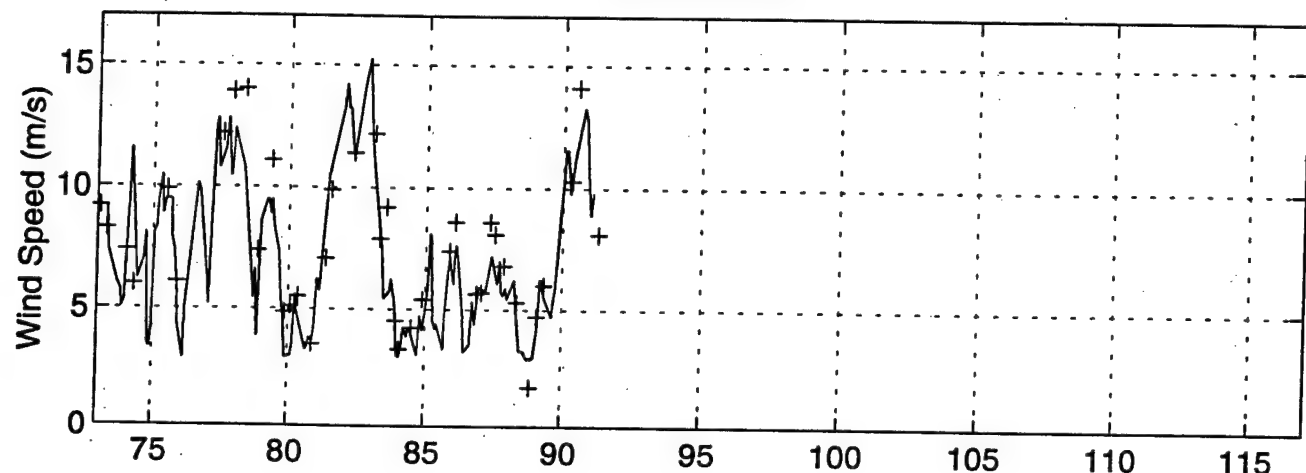


Figure 15. Atmospheric pressure, temperature and sea surface temperature for ANS Drifters #26306 (dashed line) and #26307 (solid line).

Drifter #26306



Drifter #26307

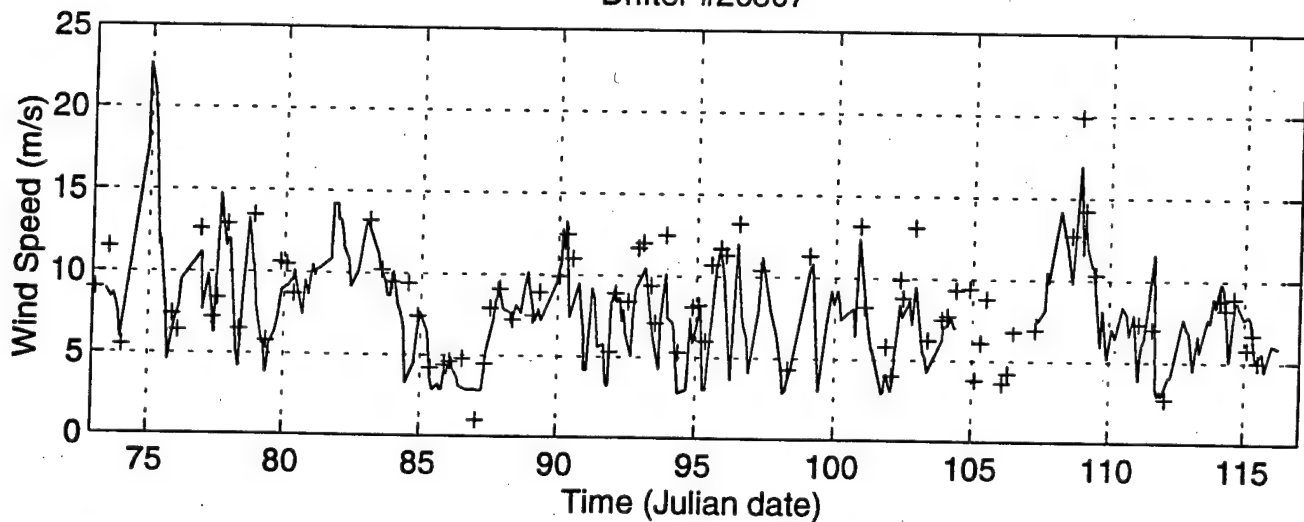
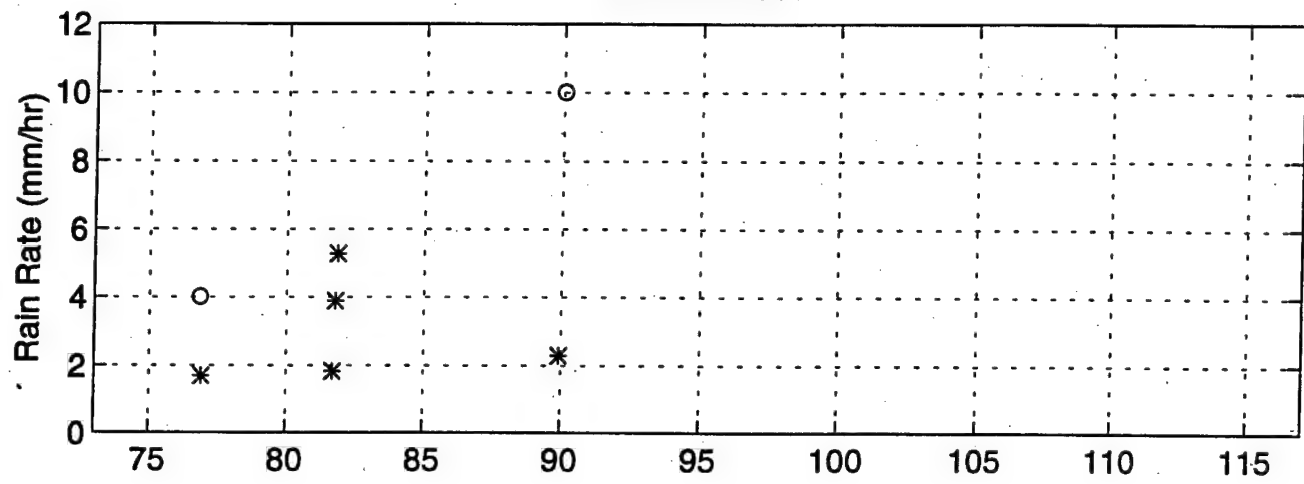


Figure 16. Acoustic (solid line) and satellite (+) wind speed comparisons for Drifters #26306 and #26307.

Drifter #26306



Drifter #26307

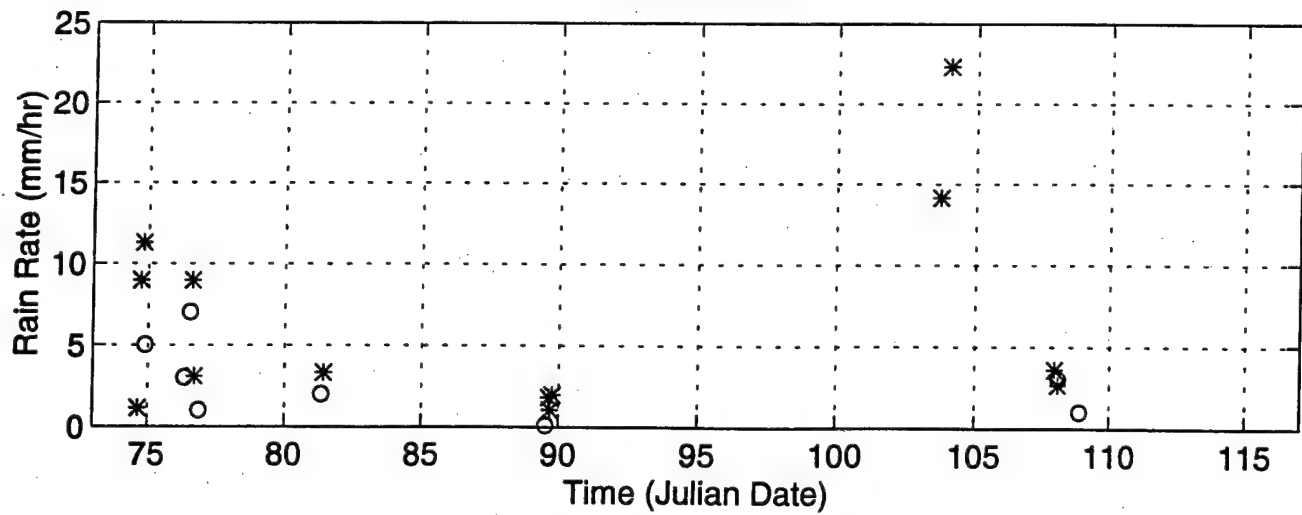


Figure 17. Acoustic (\*) and satellite (o) precipitation (drizzle and rain) detections for Drifters #26306 and #26307.

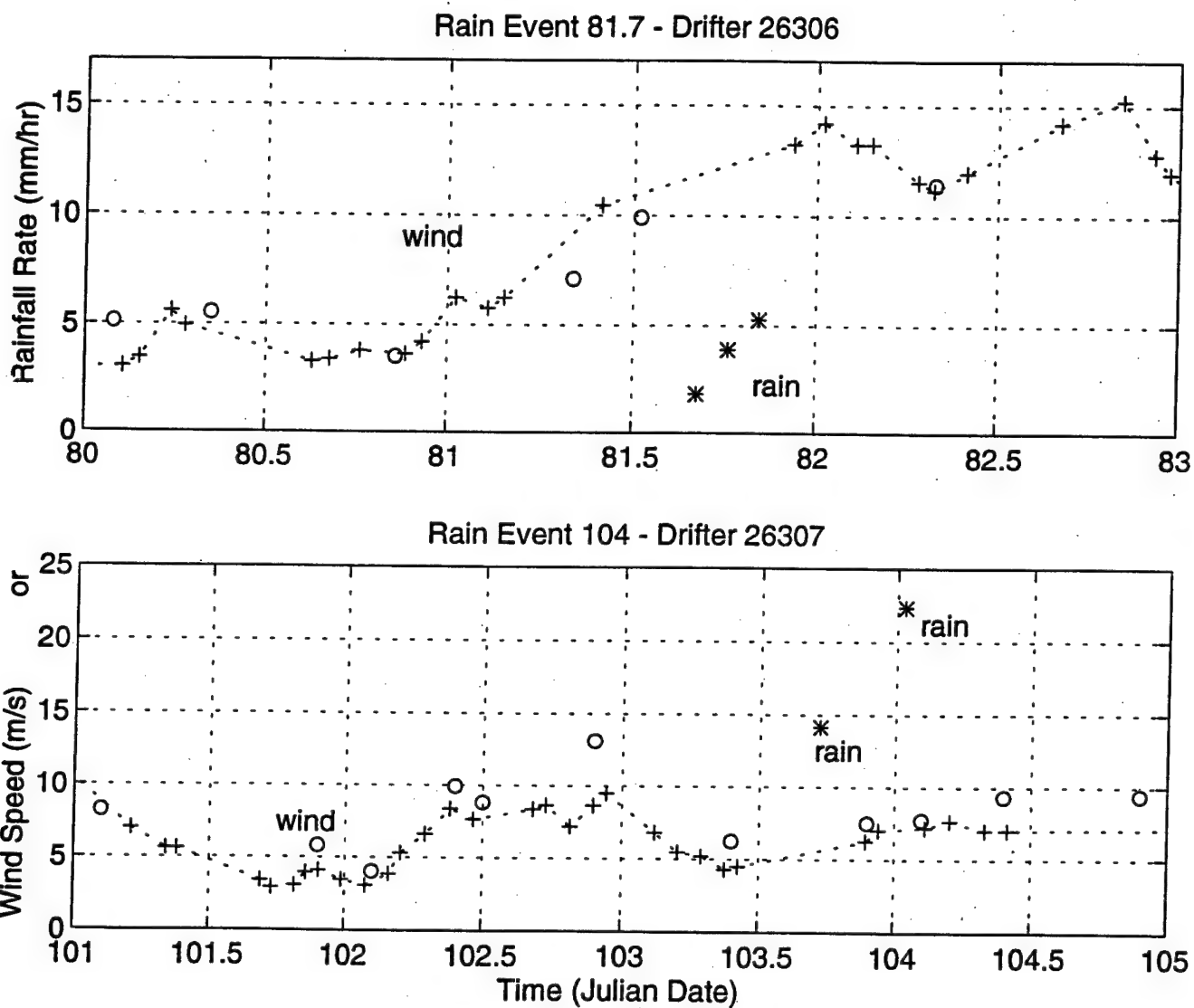


Figure 18. Two acoustic rain detections (\*) missed by the SSM/I sensors. Acoustic (+) and satellite (o) wind speed data are also shown.

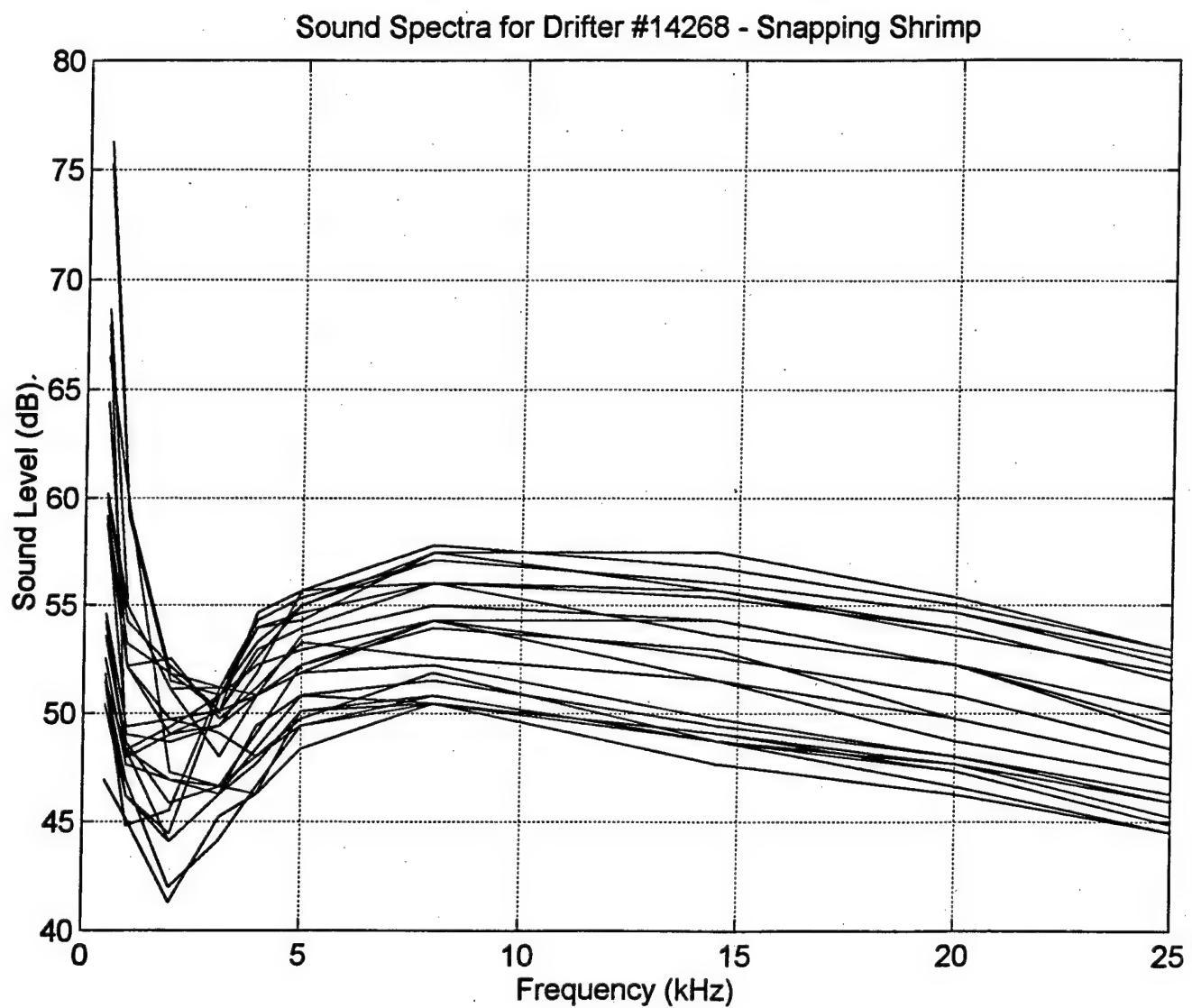


Figure 19. Sound spectra for Drifter #14268. These spectra show the characteristic shape of sound generated by snapping shrimp. This buoy was grounded on a coral reef.

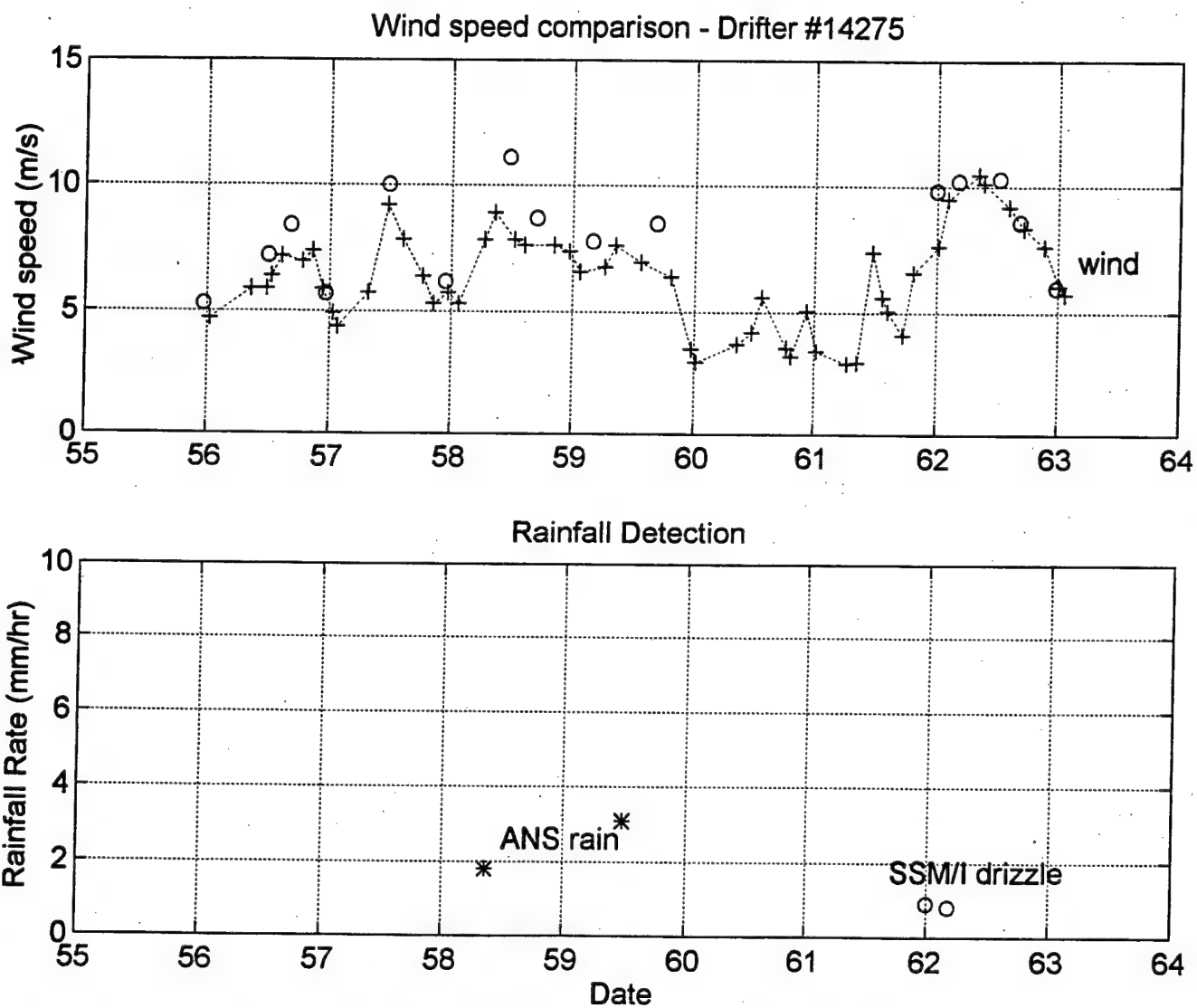


Figure 20. Wind speed and rainfall rate comparisons for Drifter #14275. Acoustic (+) and satellite (o) wind speed measurements are in the upper panel. The acoustic rain (\*) and satellite drizzle (o) detections are shown in the lower panel.

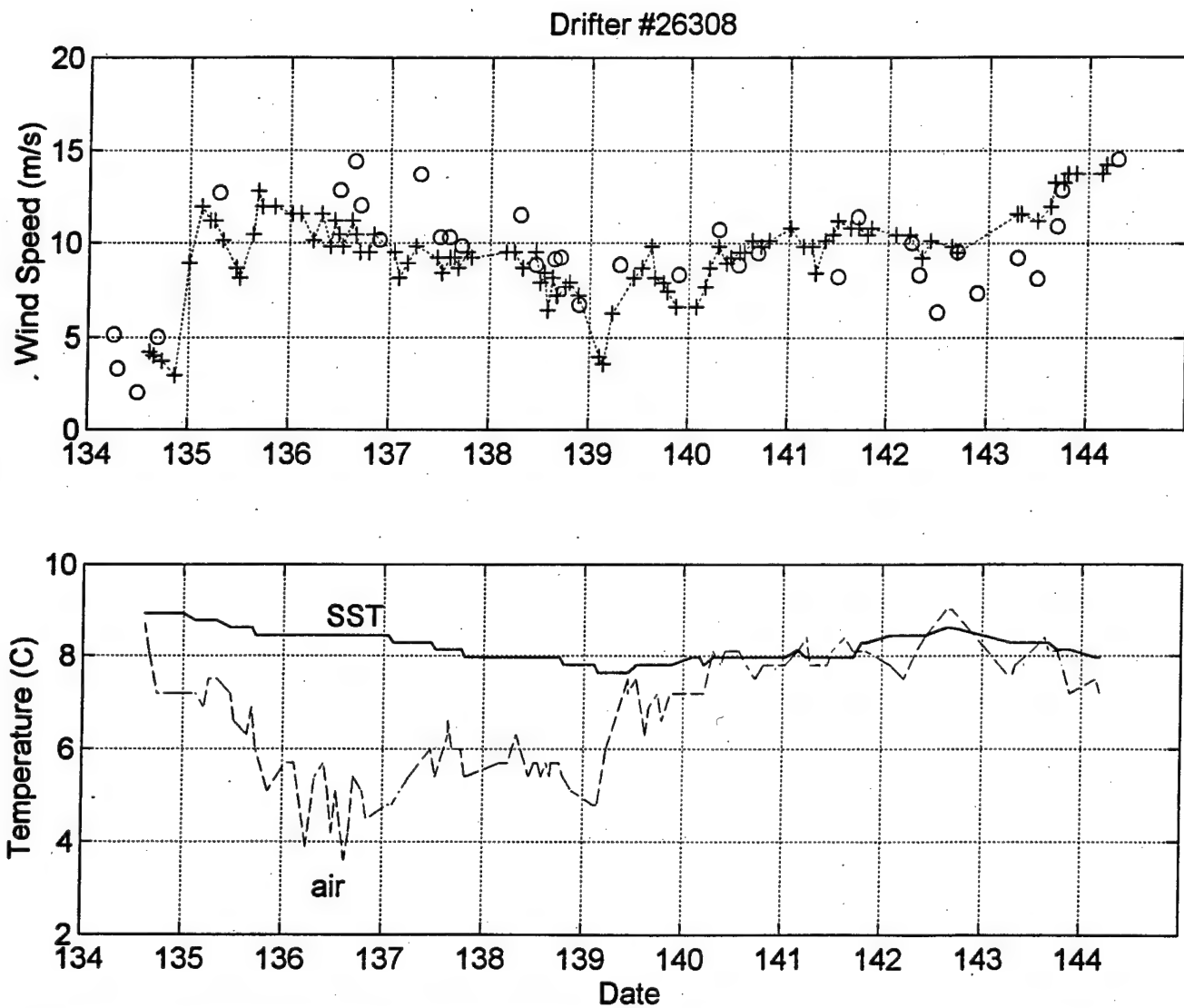


Figure 21. Environmental data for Drifter #26308. The acoustic (+) and satellite (o) wind speed measurements are shown in the upper panel. The sea surface temperature (SST) and air temperature are shown in the lower panel.

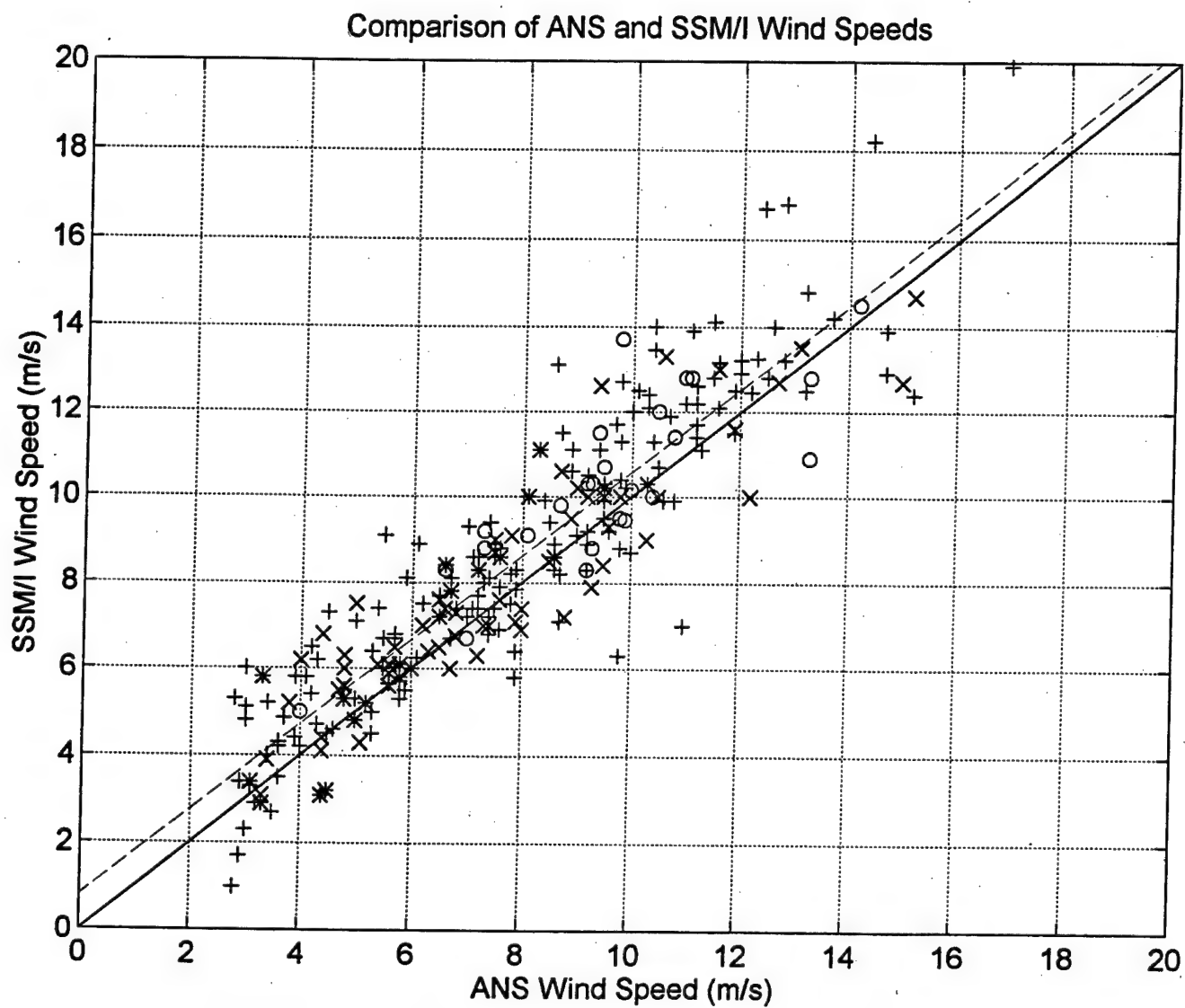


Figure 22. Comparison of ANS and SSM/I wind speed measurements. Data from the eastern North Pacific ( $\times$ ), warm water drifters ( $*$ ), the western North Pacific (+) and north of Scotland (o) show no regional or environmental trends.

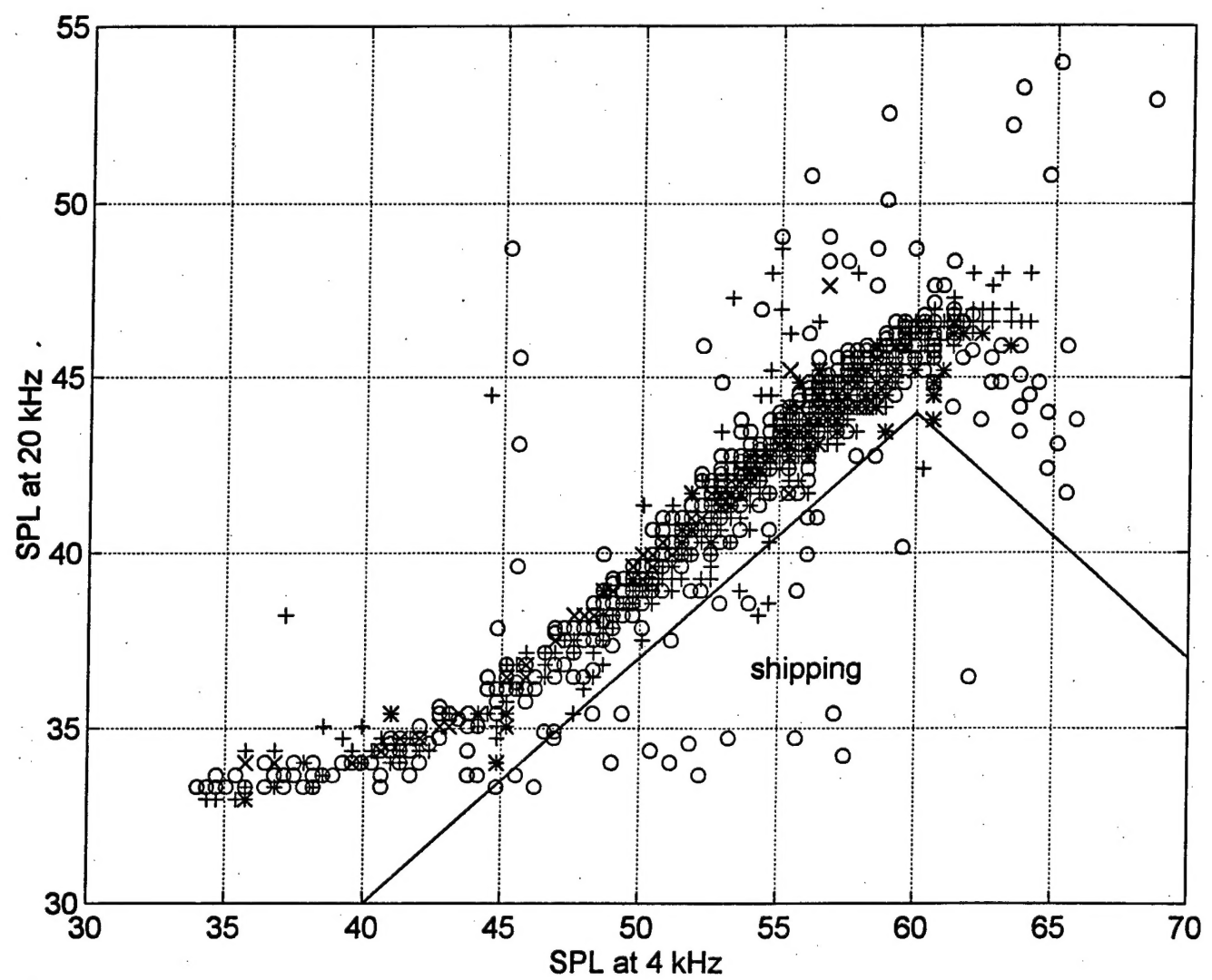


Figure A1. Shipping detection test using 4000 and 20000 Hz. Data from ANS drifters deployed in the eastern North Pacific (+), warm water (x), western North Pacific (o) and north of Scotland (\*) are shown.

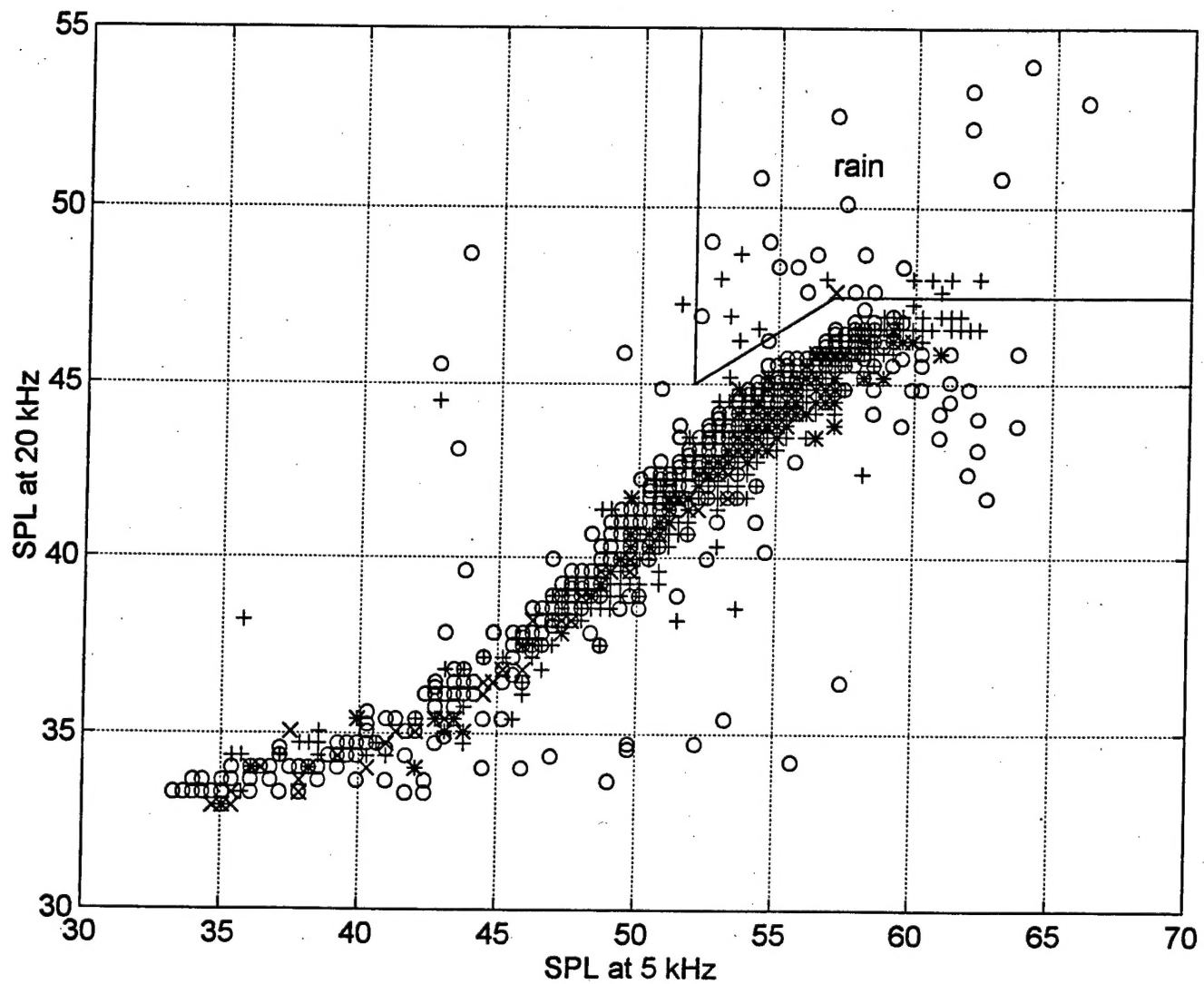


Figure A2. Rain detection test (Test #1) using 5000 and 20000 Hz. Data from ANS drifters deployed in the eastern North Pacific (+), warm water (x), western North Pacific (o) and north of Scotland (\*) are shown.

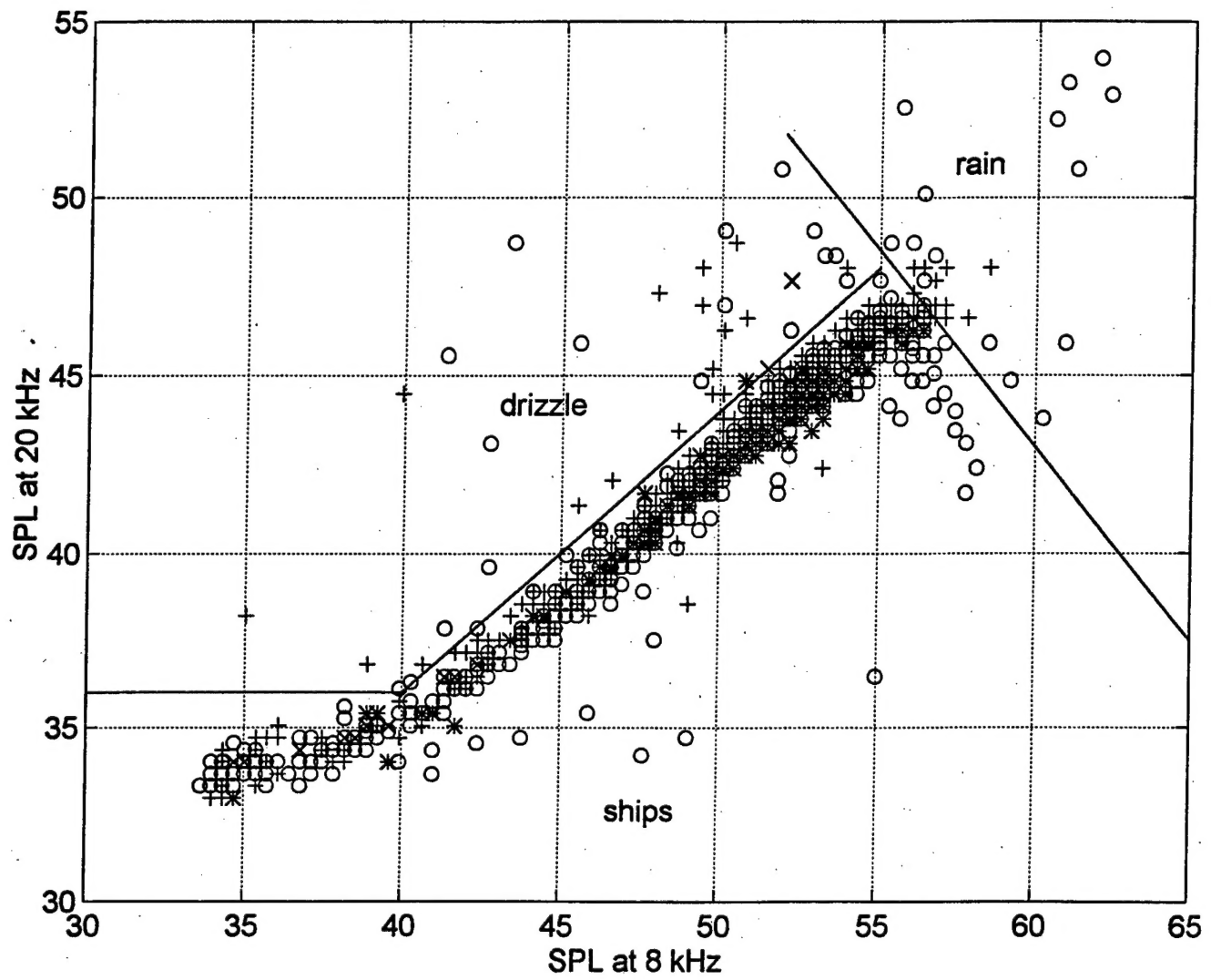


Figure A3. Rain (Test #2) and drizzle detection test using 8000 and 20000 Hz. Data from ANS drifters deployed in the eastern North Pacific (+), warm water (x), western North Pacific (o) and north of Scotland (\*) are shown. This combination of frequencies showed the least amount of regional variations in sound levels.

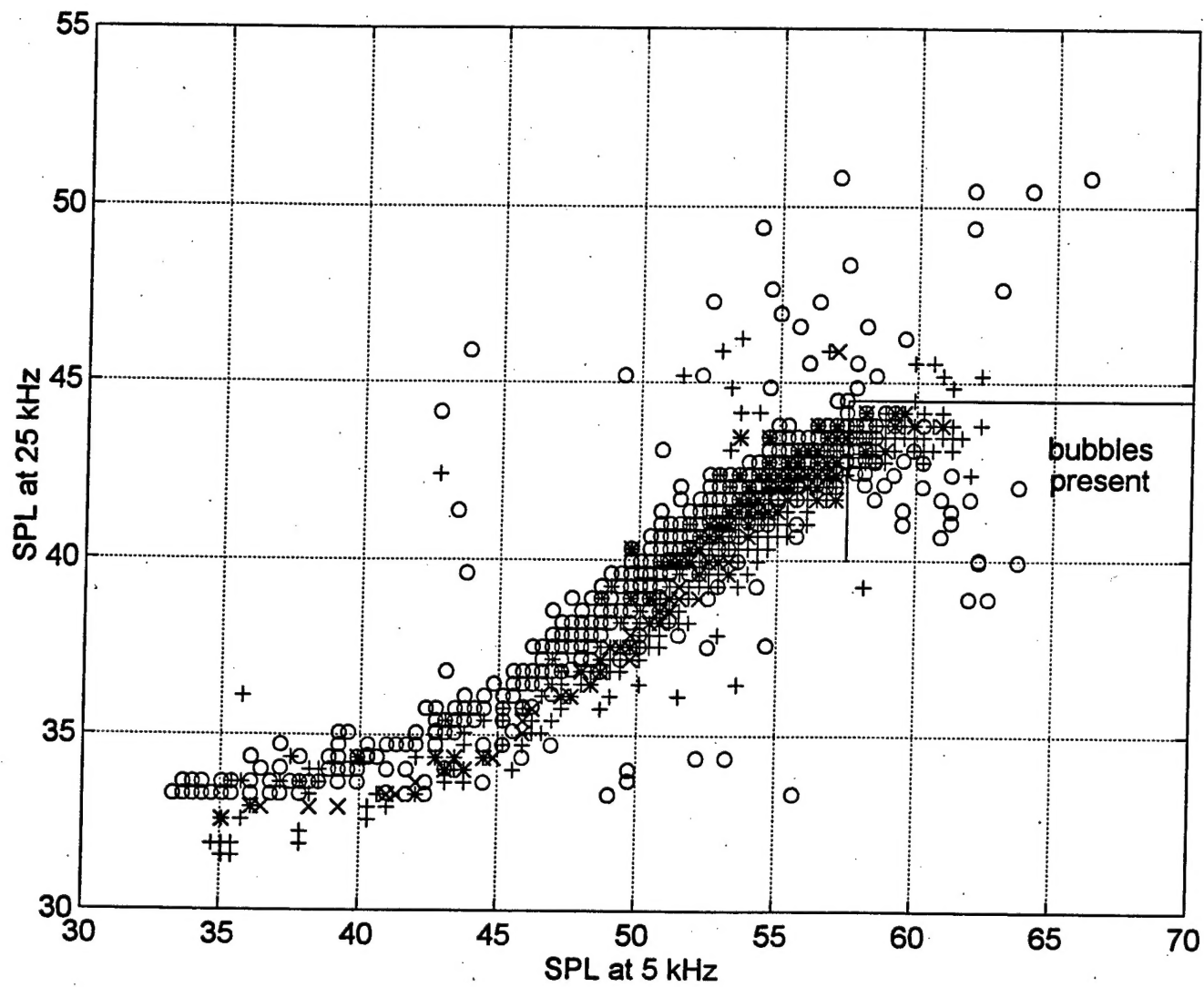


Figure A4. Bubble present test using 5000 and 25000 Hz. Data from ANS drifters deployed in the eastern North Pacific (+), warm water (x), western North Pacific (o) and north of Scotland (\*) are shown.